Estimating lockdown–induced European NO_2 changes: using satellite and surface observations and air quality models.

Jérôme Barré[1], Hervé Petetin[2], Augustin Colette[3], Marc Guevara[2], Vincent-Henri Peuch[1], Laurence Rouil[3], Richard Engelen[1], Antje Inness[1], Johannes Flemming[1], Carlos Pérez García-Pando[2,4], Dene Bowaldo[2], Frederik Meleux[3], Camilla Geels[5], Jesper H. Christensen[5], Michael Gauss[6], Anna Benedictow[6], Svetlana Tsyro[6], Elmar Friese[7], Joanna Struzewska[8], Jacek W. Kaminski[8,9], John Douros[10], Renske Timmermans[11], Lennart Robertson[12], Mario Adani[13], Oriol Jorba[2], Mathieu Joly[14], Rostislav Kouznetsov[15]

[1] European Centre for Medium-range Weather Forecast (ECMWF), Shinfield Park, Reading, UK

[2] Barcelona Supercomputer Centre (BSC), Barcelona, Spain

[3] National Institute for Industrial Environment and Risks (INERIS), Verneuil-en-Halatte, France

[4] ICREA, Catalan Institution for Research and Advanced Studies, Barcelona, Spain

[5] Department of Environmental Science, Aarhus University, Roskilde, Denmark

[6] Norwegian Meteorological Institute, Oslo, Norway

[7] Rhenish Institute for Environmental Research at the University of Cologne, Cologne, Germany

[8] Institute of Environmental Protection - National Research Institute, Warsaw, Poland

[9] Faculty of Environmental Engineering, Warsaw University of Technology, Warsaw, Poland

[10] Royal Netherlands Meteorological Institute (KNMI), De Bilt, the Netherlands

[11] Netherlands Organisation for Applied Scientific Research (TNO), Climate Air and Sustainability Unit, Utrecht, the Netherlands

[12] Swedish Meteorological and Hydrological Institute (SMHI), Norrköping, Sweden

[13] Italian National Agency for New Technologies, Energy and Sustainable Economic Development (ENEA), Bologna, Italy

[14] CNRM, Université de Toulouse, Météo-France, CNRS, Toulouse, France

[15] Finnish Meteorological Institute (FMI), Helsinki, Finland

Correspondence to: Jérôme Barré (jerome.barre@ecmwf.int)

Formatted: Correspondence

Abstract. This study provides a comprehensive assessment of NO_2 changes across the main European urban areas induced by the COVID-19 lockdown using satellite retrievals from the Tropospheric Monitoring Instrument (TROPOMI), surface site

measurements and simulations from the Copernicus Atmospheric Monitoring Service (CAMS) regional ensemble of air quality models. Some recent TROPOMI-based estimates of NO_2 changes have neglected the influence of weather variability between the reference and lockdown periods. Here we provide weather-normalised estimates based on a machine learning method (gradient boosting) along with an assessment of the biases that can be expected from methods that omit the influence of weather. We also compare the weather-normalised satellite NO_2 column changes with ~~both~~ weather-normalised surface NO_2 concentration changes and ~~simulated changes by~~ the CAMS regional ensemble, composed of 11 models, using recently published emission reductions induced by the lockdown. ~~We show that~~ Aall estimates show the same tendency on NO_2 reductions. Locations where the lockdown was stricter show stronger reductions and, conversely, locations where softer measures were implemented show milder reductions in NO_2 pollution levels. ~~Regarding~~ Aaverage reductions~~,~~ estimates based on either satellite observations (-23%), surface stations (-43%) or models (-32%) are presented, showing the importance of vertical sampling but also the horizontal representativeness. Surface station estimates are significantly changed when sampled to the TROPOMI overpasses (-37%) pointing out the importance of the variability in time of such estimates. Observation based machine learning estimates show a stronger temporal variability than the model-based estimates.

~~1.~~Introduction

1.

Nitrogen dioxide (~~NO_2) is part of the nitrogen oxides~~(NO_x; together with NO, a constituent of NO_x (~~NO_x~~=NO+NO_2) is~~and~~ a very well-established cause of poor air quality in the most urbanized and industrialized areas of the world. NO_2 is harmful for living organisms over long term atmospheric concentration exposure. It also plays a major role in urban ozone formation and secondary aerosols which are also harmful for the living at high levels in the lower atmosphere (Lelieveld et al., 2015; Myhre et al., 2013). According to the European Environment Agency (EEA 2020a) European main anthropogenic NO_x sources are road transport (39%), energy production and distribution (16%), commercial, residential and households (14%), energy use in industry (12%), agriculture (8%), non-road transport (8%) and industrial processes and product use (3%). With an atmospheric lifetime typically below 1 day, NO_x is relatively short-lived and is mainly controlled by photochemical reactions, so the majority of NO_x does not get transported far downwind from its sources (Seinfeld and Pandis, 2006). Thus, near-surface NO_x concentration is high over cities and densely populated areas and low otherwise. Besides emissions, the variability of NO_x is strongly driven by meteorological conditions, especially atmospheric transport, vertical mixing and solar radiation that can favour or not their accumulation close to emission sources (Arya, 1999). For example, increased wind speed and higher planetary boundary layer height will increase the dispersion of NO_x from the emission sources. Its short lifetime that is partly modulated by atmospheric conditions such as temperature and radiation combined with localized emission sources make NO_2 an excellent proxy for detecting emission reductions, from both surface and satellite measurements.

Formatted: Numbered + Level: 1 + Numbering Style: 1, 2, 3, … + Start at: 1 + Alignment: Left + Aligned at: 0 cm + Indent at: 0.63 cm

Formatted: Font: (Default) +Body (Times New Roman)

Formatted: Subscript

Formatted: Subscript

Formatted: Subscript

Formatted: Subscript

The worldwide outbreak of the coronavirus disease (COVID-19) that arose in late 2019 in China and spread around the world in early 2020 led many countries to take action in order to slow down the contamination growth rate of the virus. The so-called lockdowns severely restricted or banned movements of people, closed most public places and limited journeys to essential work commutes. Some measures started in China in late 2019 with stricter lockdowns in January 2020. In Europe, lockdown measures were implemented at various dates during February and March 2020. These lockdowns drastically reduced traffic and also activity levels in most industries (Guevara et al., 2020; Le Quéré et al., 2020). These sectors represent a large share of NO_x emissions (51% according to EEA 2020a). Studying NO_2 concentrations changes during the lockdown is therefore very important to assess the impact of such activity level reductions on the population pollution exposure. The COVID-19 lockdown is a unique opportunity to assess the impact of future pollution reduction measures, in particular the impact of drastic reductions on the road transport sector using combustion energy.

The lockdowns are expected to have large effects on urban NO_2 air pollution levels in conjunction with other modulating factors (i.e., weather conditions). The first quarter of 2020 had specific and highly variable meteorological conditions. The storm Ciara crossed over Europe in the second week of February followed by the Storm Dennis that also crossed Europe a week later. Both extratropical storms generated strong winds over the northern half of Europe (above 45°N) from February 9th, 2020 until February 18th, 2020. Strong wind situations, yet milder, over the Iberian Peninsula, the southern part of France and the northern part of Italy were also generated by Storms Karine and Myriam in the first week of March. Moreover, February and March 2020 displayed stronger positive temperatures anomalies over Europe in comparison with February and March 2019 (https://surfobs.climate.copernicus.eu/stateoftheclimate). Such weather anomalies however did not persist further during the second quarter of 2020. Accounting for the effect of such meteorological variations is very important to assess accurately the effect of COVID-19 related mobility restrictions on air pollution. Different approaches can be used to assess such pollution changes, based on different types of data such as: satellite observations, surface site observations and air quality models.

Several studies used the recently launched (October 2017) Tropospheric Monitoring Instrument (TROPOMI, Veefkind et al., 2012) on board the Copernicus Sentinel-5 Precursor (S5P) satellite to showcase the NO_2 reductions caused by the COVID-19 lockdowns. Due to the substantial interannual variability of meteorological conditions, the young age of the instrument prevents estimating a representative climatological baseline to be compared to NO_2 levels observed during the lockdown period. Satellite based studies using TROPOMI comparing before and after lockdown periods (e.g., Wang et al., 2020b) or comparing the lockdown period with its 2019 equivalent (e.g., Bauwens et al., 2020, Nakada et al., 2020, Zambrano-Monserrate et al. (2020)) give little to no weight to the synoptic meteorological conditions and how they could potentially flaw the pollution change estimates.

In contrast, Schiermeier (2020) mentioned the 'weather factor' early on in the COVID-19 crisis which can affect strongly the pollution levels. And studies as for example Le et al. (2020) showed 2019 and 2020 TROPOMI NO_2 comparisons but acknowledged the impact of weather anomalies on pollution levels. Only very recently a weather-normalisation technique has been applied to estimate NO_2 changes due to the COVID-19 restrictions across cities in the US based on TROPOMI

Formatted: Subscript

Formatted: Font: (Default) Times New Roman, Font colour: Auto

Formatted: Subscript

(Goldberg et al., 2020). Also, insufficient importance and clarity are given about the fact that satellite data used in such analyses are conditioned by the cloud coverage, revisit frequency and quality flag. Ignoring or not acknowledging such information can also lead to flawed satellite based estimates and provide misleading information (https://atmosphere.copernicus.eu/flawed-estimates-effects-lockdown-measures-air-quality-derived-satellite-observations).

A number of studies used surface in-situ measurement ~~sites~~. For example, Wang et al. (2020a) showed that lower emissions from motor vehicles and secondary industries were most likely responsible for the observed decreases of NO_2 concentrations in China during January-March 2020. Collivignarelli et al. (2020) showed using surface station measurements that major NO_2 reductions occurred in Milan, a city that showed rapid increase of cases early in the European COVID-19 crisis (February 2020) and was one of the first cities to be put into lockdown in Europe. Past studies such as Carslaw and Taylor (2009) showed the usefulness and the importance of weather normalisation techniques for air pollution applications using surface observations, such as local air traffic activity impact on NO_2 predictions. This was followed more recently by Grange et al. (2018, 2019) where machine learning techniques were used to perform weather normalisation for analysing trends and detecting the impact of policy measures on air quality. Built on this previous work, several studies made use of machine learning to estimate the impact of the COVID-19-related mobility restrictions on air pollution levels, taking into account the confounding effect of the meteorological variability. Using ML models fed with ERA5 reanalysis meteorological data, ~~Accounting for the effect of the meteorological variability,~~ Petetin et al. (2020)~~.~~ highlighted a strong reduction of surface NO_2 concentrations across most Spanish urban areas during the first weeks of lockdown. Similarly, Keller et al., 2020 assessed the NO_2 pollution changes using surface measurements globally showing country dependent variations on reductions.

Finally, ~~The first quarter of 2020 had specific and very changing meteorological conditions. The storm Ciara crossed over Europe in the second week of February followed by the storm Dennis that also crossed Europe a week later. Both extratropical storms generated strong winds over the northern half of Europe (above 45°N) from February 9th, 2020 until February 18th, 2020. Strong wind situations, yet milder, over the Iberian Peninsula, the southern part of France and the northern part of Italy were also generated by storms Karine and Myriam in the first week of March. Moreover, February and March 2020 displayed stronger positive temperatures anomalies over Europe in comparison with February and March 2019 (https://surfobs.climate.copernicus.eu/stateoftheclimate). Such weather anomalies however did not persist further during the second quarter of 2020.~~ ~~a~~Air quality modelling ~~prediction~~ systems offer a valuable tool for ~~-~~ representing the evolution of pollutants in the atmosphere according to changes in emissions, physical processes and weather variability~~accounting for changes in weather using numerical weather prediction data~~. The Copernicus Atmospheric Monitoring Service (CAMS) produces European air quality forecasts and analyses daily using an ensemble of 11 models and the European Centre for Medium-range Weather Forecasts (ECMWF) data as input ensuring unique reliability and quality (Marecal et al., 2015). Using scaling emission factors to account for lockdown measures such an ensemble of models~~system~~ can be used to estimate lockdown reductions on NO_2 pollution (amongst other pollutants) and account for the weather variability (Colette et al., 2020, Guevara et al., 2020).

Formatted: Subscript

Formatted: Subscript

Several studies used the recently launched (October 2017) Tropospheric Monitoring Instrument (TROPOMI, Veefkind et al., 2012) on board the Copernicus Sentinel-5 Precursor satellite to showcase the NO_2 reductions due to the COVID-19 lockdown. Due to the young age of the instrument it is impossible to work with a climatological baseline that would use at least several years to assess the lockdown reductions. Zambrano-Monserrate et al. (2020)A number of TROPOMI NO_2 studies on COVID-19 lockdown reductions give little weight to the synoptic meteorological conditions and how they could potentially flaw the estimates.Often satellite data from 2020 are compared with data from 2019 sometimes over short time periods. For example, Muhammad et al. (2020), compared full March 2019 averages with the 14-25 March 2020 average for Europe, amongst other estimates for other regions. Bauwens et al. (2020) provided a more in-depth assessment of NO_2 column reduction estimates by using similar year to year methodology, i.e. comparing 2019 to 2020. A number of TROPOMI NO_2 studies on COVID-19 lockdown reductions give little weight to the synoptic meteorological conditions and how they could potentially flaw the estimates. Zambrano-Monserrate et al. (2020) and Nakada et al., (2020) showed maps of TROPOMI for short time periods comparing 2020 with 2019 for Europe, Asia and South America with no clear quantitative and robust assessment of the underlying weather conditions. Wang et al. (2020b), used differences of TROPOMI NO_2 images over China before and during the lockdown to illustrate the impact of the lockdown on air pollution, but do not emphasise on how those differences might be affected by differences in weather conditions. In contrast, Schiermeier (2020) mentioned the 'weather factor' early on in the COVID-19 crisis which can affect strongly the pollution levels. And studies as for example Le et al. (2020) showed 2019 and 2020 TROPOMI NO_2 comparisons but acknowledged the impact of weather anomalies on pollution levels. Only very recently a weather-normalization technique has been applied to estimate NO_2 changes across cities in the US based on TROPOMI (Goldberg et al., 2020). Also, insufficient importance and clarity are given about the fact that satellite data used in such analyses are conditioned by the cloud coverage, revisit frequency and quality flag. Ignoring or not acknowledging such information can also lead to flawed satellite based estimates and provide misleading information (https://atmosphere.copernicus.eu/flawed-estimates-effects-lockdown-measures-air-quality-derived-satellite-observations).

TIn this paper , we aims atto providing a comprehensive and comparative assessment of the impact of the first European COVID-19 lockdown on NO_2 pollution levels over major European urban areas using: satellite observations, surface in-situ observations and air quality models. We firstly illustrate how misleading it can beis to ignore the influence of the weather variability when assessing the lockdown-induced changes of NO2 with TROPOMI. Then, in order to quantify these changes, we use ML-based weather-normalisation methods for estimating the "business as usual" (BAU) NO_2 pollution levels that would have been observed without any lockdown measures, based on both TROPOMI NO_2 tropospheric columns (Sect. 2) and surface in-situ observations (Sect. 3). NO_2 changes are then investigated with the CAMS regional ensemble (Sect. 4). We compare and discuss the three different approaches in Sect. 5 followed by conclusions in Sect. 6.

consider non-weather normalized TROPOMI estimates for assessing changes in NO_2 induced by lockdown measures. We focus on Europe and provide a method that accounts for weather variability or more broadly speaking estimates what TROPOMI would have measured in Spring 2020 under "business as usual" (BAU) emission forcing (i.e. without any lockdown measures) in section 2. We then aim to provide a comprehensive assessment of the European lockdown induced NO_2 changes.

Formatted: Subscript

Formatted: Subscript

Formatted: Subscript

Formatted: Subscript

~~We compare the satellite estimates against what can be inferred from surface observations that also account for weather variability in section 3. We compare also with model-based scenarios using ad hoc bottom-up emission inventories reflecting lockdown restrictive measures in section 4. We summarize and confront all the presented estimates in section 5.~~

2. TROPOMI NO_2 column estimates~~changes~~

2.1. Dataset and analysis periods

We use the operational Copernicus ~~Sentinel-5 Precursor (~~S5P~~)~~ TROPOMI NO_2 level 2 product, for which data have been available since 28 June 2018. These observations are tropospheric columns (from the surface to the top of the troposphere) with a pixel resolution of 5.5km by 3.5km since 6 August 2019 and 7km by 3.5km before. The instrument can have up to daily revisit at 13:30 mean local solar time upon clear sky condition. ~~and in this study,~~ The quality ~~we are making use of a quality~~ flag (qa) provided with the retrieval is used to select only good quality data (qa > 0.75), which ~~the so called "qa" flag, and only selecting good quality data, i.e. qa > 0.75. This~~ removes cloud-covered scenes, errors and problematic retrievals (Eskes et al., 2019). TROPOMI data are binned ~~We have binned the data~~ on a regular 0.1° × ~~x~~0.1° grid in order to perform statistical analyses and to facilitate the processing of timeseries for locations of interest, i.e., large European cities in this study (see section 2.2) as well as the comparison with other datasets such as the 0.1° × 0.1° ~~0.1°x 0.1°~~ CAMS regional air quality models (Marecal et al., 2015) and the 9 km European Centre for Medium range Weather Forecasts (ECMWF) weather forecasts.

In this study we consider February, March and April 2020 and 2019 to ~~assess the changes seen in TROPOMI~~ NO_2 columns due to COVID-19 restrictions over Europe. ~~Even~~ Although the lockdown conditions and dates vary between countries, the~~after~~ 15 March 2020 is here considered as a representative starting date of the European-wide lockdown, given that most European countries implemented their nation-wide social distancing measures along the 2-week period going from ~~can be considered as a European lockdown as in the middle of the approximate 2-week transition period (e.g.~~ 9 March 2020 ~~(in~~ Italy~~)~~ to~~and~~ 23 March 2020 ~~in the~~ (United Kingdom (UK)). Two periods of the year are considered in this study: the pre-lockdown period going from 1 February to 15 March, and the lockdown period going from 16 March to 31 April. This study thus focuses on the most stringent period of the first European lockdown (since many countries then started to ease up their lockdown restrictions from the beginning of May onwards).

~~We choose to limit our comparisons to the period up to the end of April as a large portion of countries eased up their lockdown restrictions from the beginning of May onwards. To have an equivalent pre-lockdown period we then include 1 February until 15 March. Table 1 summarizes the periods considered in this study.~~

~~Pre-lockdown~~	~~Lockdown~~
~~From 1 February until March 15~~	~~From March 16 until April 30~~

Formatted: Indent: First line: 0 cm
Formatted: Indent: First line: 1.27 cm
Formatted: Subscript
Formatted: Indent: First line: 0 cm
Formatted: Justified
Formatted: Justified

~~**Table 1. Definition of the 2020 pre-lockdown and lockdown period over Europe considered in this study. Same dates are used for 2019 to perform the comparisons.**~~

In Figure 1, mean TROPOMI NO_2 tropospheric columns ~~the 0.1°x0.1° binned averages~~ are displayed for the pre-lockdown and lockdown periods in 2020 and their equivalents in 2019. The comparison of pre-lockdown and lockdown averages for 2020 only shows a decrease in Southern Europe but no clear reduction over more Northern latitudes (i.e., the ~~United Kingdom (~~UK~~)~~, T~~T~~he Netherlands and Germany). In the corresponding 2019 pre-lockdown period much larger NO_2 columns ~~than in 2020~~ are seen compared to 2020~~found~~. During this period of the year, the meteorological conditions over Northern Europe in 2019 and 2020 were significantly different. A number of named extratropical cyclones (Storms Ciara, Denis, Karine and Myriam) combined with a strong positive anomaly in temperature occurred over Europe during February and early March 2020~~,~~ especially Western and Northern Europe.~~,~~ ~~in February and early March 2020, while no s~~Such anomalies in wind and temperature were not observed in 2019. Figure 2 shows the distribution of 10-meter wind speed, ~~and~~ planetary boundary layer (PBL) height and 2-meter temperature ~~from~~ the 9 km operational forecasts from the ECMWF Integrated Forecasting System (IFS) in both 2019 and 2020 for the pre-lockdown and lockdown periods at the S5P overpass times. Detail on how the PBL height is calculated can be found in the IFS documentation (part IV, chapter 3 in https://www.ecmwf.int/en/elibrary/19748-part-iv-physical-processes). Before 15 March, these~~The two~~ parameters show very different distributions before 15 March, with much lower values in 2019 than in 2020, i.e., less circulation and less vertical dilution with colder conditions ~~of NO_2~~. Such differences in meteorological conditions lead~~ing~~ to an increase of ~~d~~ NO_2 tropospheric columns in 2019 compared to 2020. Conversely, d~~D~~uring the post-15 March period, the meteorological distributions are more similar ~~but still~~ showing ~~some~~ much less differences. This illustrates the potential need for accounting for the meteorological effect when assessing the changes of NO_2 tropospheric columns associated with the lockdown.

Formatted: Justified, Indent: First line: 0 cm

Formatted: Indent: First line: 0 cm

Formatted: Subscript

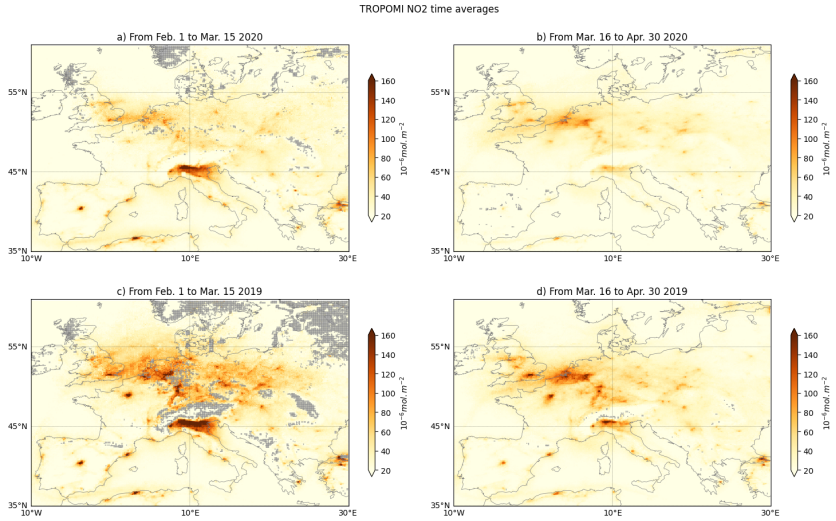

Figure 1. Average maps of the TROPOMI NO_2 tropospheric columns (mol.m^{-2}) for European pre-lockdown and lockdown periods in 2020 (a, b respectively) and corresponding periods in 2019 (c, d). Grey areas indicate where the number of revisits is strictly below 5.

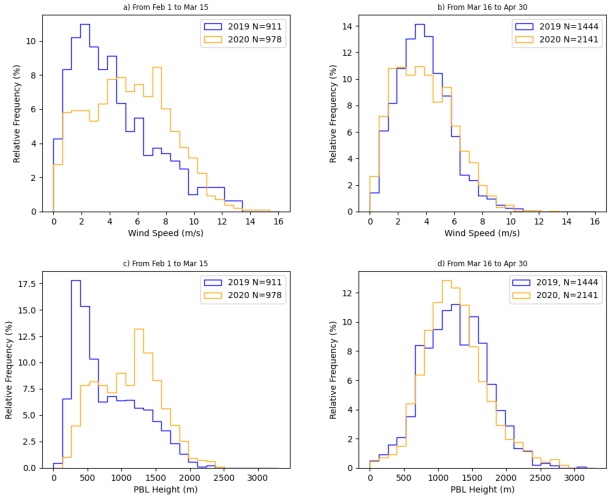
a) From Feb 1 to Mar 15
2019 N=911
2020 N=978
Relative Frequency (%)
Wind Speed (m/s)
b) From Mar 16 to Apr 30
2019 N=1444
2020 N=2141
Relative Frequency (%)
Wind Speed (m/s)
c) From Feb 1 to Mar 15
2019 N=911
2020 N=978
Relative Frequency (%)
PBL Height (m)
d) From Mar 16 to Apr 30
2019, N=1444
2020, N=2141
Relative Frequency (%)
PBL Height (m)

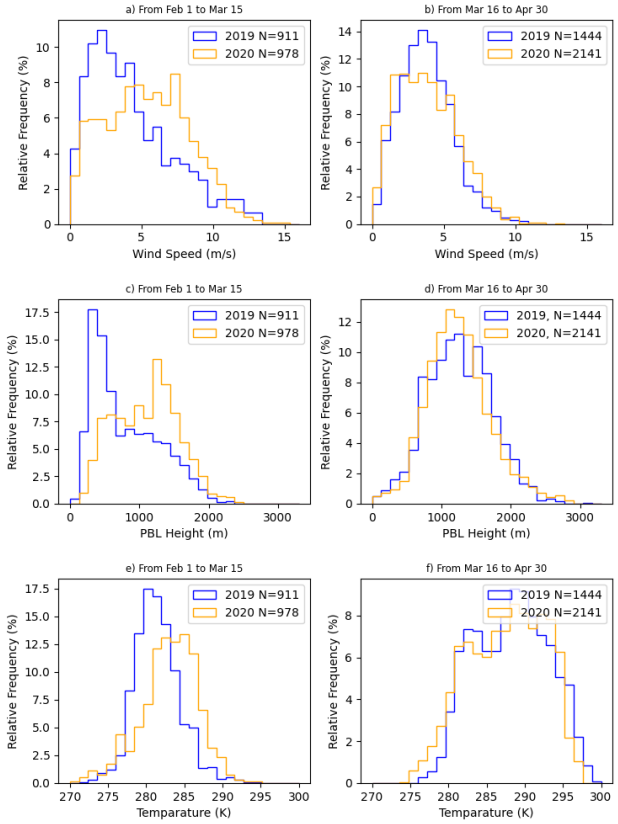

220

Figure 2. Probability density functions of 10-meter wind speed (m.s^{-1}, first row~~top~~), ~~and~~ planetary boundary layer (PBL) height (m, ~~bottom~~second row), and 2-meter temperature (K, third row) from the ECMWF operational forecasts for European periods before (a,b) and after 15 March (c,d), comparing 2020 to 2019. Distribution ~~are~~is computed for urban areas above 0.5 Million inhabitants between 10°W,20°E,45°N and 60°N at the S5P overpasses

225 **times. N is the sample size for each distribution that can be multiplied by the relative frequency (in %) to obtain the absolute frequency.**

2.2. Non- weather normalised changes of TROPOMI NO_2 tropospheric column ~~changess estimates~~

Changes of NO_2 tropospheric columns associated with the lockdown measures can be estimated by comparing NO_2 levels observed during the lockdown period in 2020 with a given baseline. In this section, we compare the results obtained with two~~hree~~ different baselines~~:~~ (1) the NO_2 levels observed during the pre-lockdown period in 2020 (hereafter referred to as the "before-during" approach), (2) the NO_2 levels observed during the same period of the year in 2019 (hereafter referred to as the "year-to-year" approach)~~, and (3) an machine learning-based estimate of the business-as-usual NO_2 levels that would have been observed during the lockdown period in 2020 in the absence of lockdown measures.~~ We focus our study on largest European urban areas where the city population is exceeding 0.5 million inhabitants (according to the population database provided by https://simplemaps.com/data/world-cities), making a total of 100 locations. Assessing the changes of NO_2 tropospheric columns from satellite observations is more challenging over rural areas as the NO_2 levels are much lower than over urban areas. Signal to noise ratio is significantly low in rural areas thus estimates are very sensitive to small changes in the tropospheric columns. ~~We use the TROPOMI NO_2 re-gridded 0.1° x 0.1° averages filtered according to relevant quality flags (see section 2.1)~~We ~~and~~ choose the pixels closest to the European city centres and that have more than 5 data points per pre-lockdown and lockdown period. If this condition is not reached, the location is discarded from the analysis. ~~defined in Table 1. We first show the reduction estimates over Europe as calculated by examples of non-weather-normalized estimates.~~ The "before-during" estimate corresponds to the difference between pre-lockdown and the lockdown periods median estimates. Figure 3 shows changes calculated in that way for 2020 (Fig. 3b) and equivalent in 2019 (Fig 3a) for comparisons. This method shows drastic NO_2 reductions, by~~of~~ more than 75% in 2020 for most of the Southern European large urban area~~ss of Southern Europe~~. Reductions are not obvious over ~~some of~~ N~~N~~orthern Europe~~an urban areas~~ and show strong variations from one location~~ity~~ to another. For example, over the UK and Germany some urban areas show increases well above 30% while other urban areas show reductions even though the same lockdown measures were applied nationwide. A~~A~~pplying the same method over~~to~~ 2019 ~~data, from 2019~~ is showing as strong decrease~~s~~ of NO_2 levels over~~in~~ many major European urban~~ areasareas between the corresponding pre-lockdown and lockdown periods~~. Such reductions in 2019 are obviously not expected. For these reasons, ~~This illustrates that~~ such "before-during" type of satellite estimates~~comparisons~~ do not provide a robust methodology ~~is misleading and unfit~~ for assessing the effects of COVID-19 lockdown on European NO_2 pollution levels. ~~because it is very sensitive to seasonal variations of weather regimes and emissions.~~

Formatted: Font: (Default) Times New Roman

Formatted: Font: (Default) Times New Roman

Formatted: Font: (Default) Times New Roman

Formatted: Font: (Default) Times New Roman

Formatted: Subscript

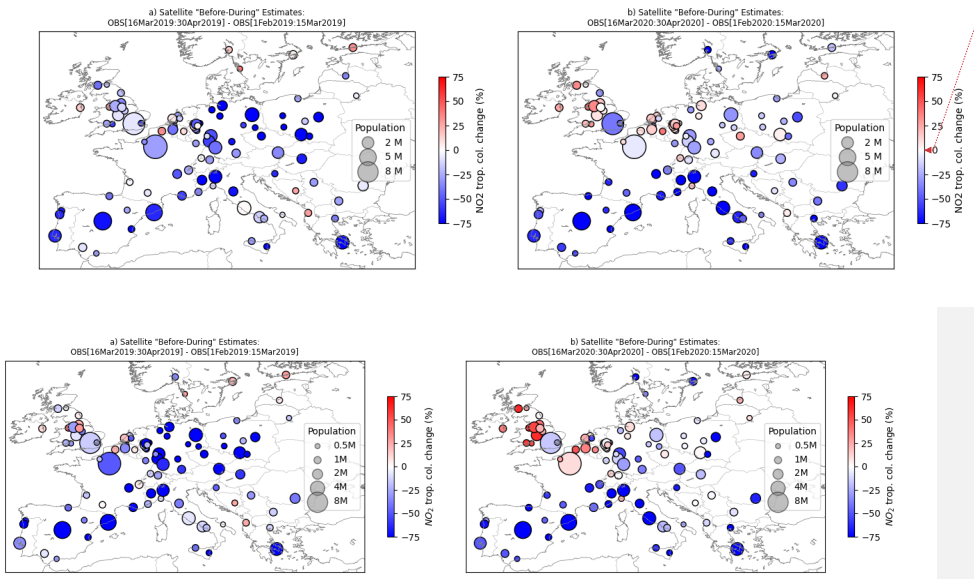

Figure 3. "Before-during" estimates of **TROPOMI** ~~based estimates of~~ **tropospheric NO_2 column change (%) for urban areas above 0.5 million inhabitants**, in 2019 (a) and 2020 (b). ~~computed using pre-lockdown period (from 1 Feb. to 15 Mar.) and lockdown period (from 16 Mar. to 30 Apr.) comparison for 2019 and 2020 (a and b respectively).~~ **The diameter of the circles is proportional to the population count in each urban area.**

The "year-to-year" approach has been more widely used in scientific publications and web press releases and consists in ~~is based on~~ comparing 2020 to 2019 data over the period of interest. Figure 4 shows such "year-to-year" estimates, comparing the median values between 2020 and 2019, for the pre-lockdown (Fig. 4a) and lockdown (Fig. 4b) periods. During the lockdown an overall reduction is seen all over Europe with more moderate reductions over Southern Europe ~~as~~ compared to the "before-during" estimates (see Fig.~~ure~~ 3b). Northern Europe changes do not show strong ~~city dependent~~ variations between urban areas as in the "before-during" method. ~~and~~ An overall decrease is seen over most European locations, with strongest reductions ~~that is not as strong as~~ in ~~Southern~~ European countries (e.g., France, Spain or Italy) where lockdown measures were more stringent (according to the Oxford Coronavirus Government Response Tracker stringency index Hale et al., (2020)). However, looking at the pre-lockdown estimates, Northern Europe also shows drastic negative changes, that are

Formatted: Justified, Indent: First line: 0.63 cm

actually larger than during the lockdown period., ~~where~~ ~~S~~such deviations in pollution levels across Europe ~~from the BAU levels~~ should not be expected in the case of attributing the impact of emission changes. The "year to year" method thus appears to be ~~is~~ strongly dependent on the interannual NO_2 variability ~~even in the BAU situation~~, where meteorology plays a crucial role. Although it respects the seasonality on NO_2~~Therefore, ,~~ this method could still~~an~~ lead to large errors when assessing differences in NO_2 levels and more generally the pollution level reductions due to the COVID-19 lockdown.

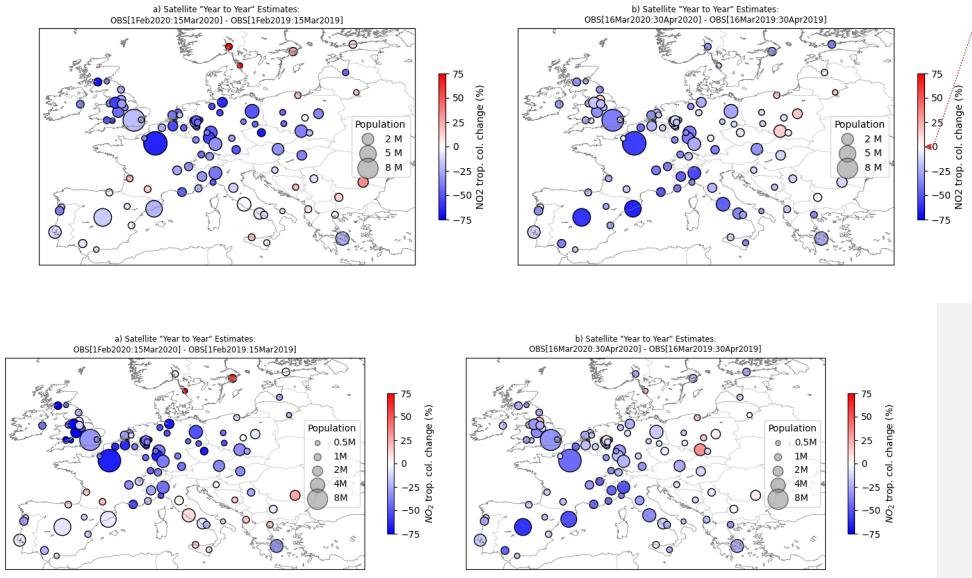

Figure 4. "Year-to-year" estimates of TROPOMI tropospheric NO_2 column change (%) for urban areas above 0.5 million inhabitants, in 2019 (a) and 2020 (b). ~~Satellite observation estimation of tropospheric NO_2 column change (%) for urban areas with at least 0.5 million inhabitants computed using 2019 and 2020 ("year to year") comparison for the pre-lockdown and lockdown periods (a and b respectively).~~ **The diameter of the circles is proportional to the population count in each urban area.**

Formatted: Subscript

Formatted: Justified, Indent: First line: 0.63 cm

2.3. Weather normalised changes of TROPOMI NO_2 tropospheric column ~~changess~~ ~~estimates~~

2.3.1. Methods

The weather-normalisation method accounts for weather variability to estimate the net changes of NO_2 induced by the lockdown in urban areas. We have simulated NO_2 tropospheric columns as TROPOMI would have measured in BAU conditions for 2020, i.e., in the absence of lockdown restrictions. Using meteorological and air pollution predictors to build a simplified model for satellite tropospheric observation simulations or predictions for atmospheric composition have been used in previous studies (e.g., Worden et al., 2013, Barré et al., 2015). In this study, we use a novel approach for satellite observation simulation based on the Gradient Boosting Machine (GBM, Friedman, 2001) regressor technique. GBM is a popular decision tree-based ensemble method belonging to the boosting family. We use weather and air quality variables as predictors from the ECMWF and CAMS operational forecasts at 9 km and 0.1° resolutions respectively: 10-m wind speed and direction, PBL~~planetary boundary layer~~ height, 2-m temperature, surface relative humidity, geopotential at 500hPa, NO_2 surface concentrations from the CAMS regional ensemble forecasts. The NO_2 surface concentrations used here are obtained from the CAMS operational regional forecasts which (~~is~~ business as usual information and are a different output from the simulations presented in section 4. In the CAMS forecasts product, no assimilation is performed and BAU emissions are used. Therefore, the NO_2 surface concentrations used to train and make model predictions do not include lockdown effects and then are independent form the air quality model pollution changes estimates provided in section 4.) Additional, time and location parameters were also included in the set of predictors:~~but also~~ latitude, longitude, population, Julian date (number of days since January 1st) and weekday (to reflect expected weekend/weekday effects). Quite similar machine learning (ML)-based approaches have already been successfully applied to in-situ surface AQ observations (e.g., Grange et al., 2018, 2019, Petetin et al., 2020). We use data from 1 January 2019 to 31 May 2019 as a training set and apply the model on 2020 to generate ~~BAU~~ predictions of BAU NO_2 tropospheric columns. For validation purposes we have randomly split the data in a 90% and 10% share for training and test, respectively. We then train the model on using the training set only and leaving the test set for final evaluation. Hyper-parameter tuning (see annex A for details) was performed using a grid search method with 5-fold cross-validation and using the ranges indicated by Petetin et al. (2020) ~~that set up a similar method using surface stations~~. In contrast ~~Contrary~~ to Petetin et al. (2020) that trained one ML model per surface air quality monitoring station, only one single ML model is trained here for all cities. This choice is motivated, ~~by due to~~ the small size of the dataset available (about 10,000 data points, see Table 1~~2~~). After the hyperparameter tuning and evaluation of the model, the observation BAU predictions have been generated using 100% of the January-May 2019 dataset in order to use the maximum amount of data points possible.

MB	nMB	RMSE	nRMSE	PCC	N
[10^{-6}mol.m^{-2}]	[%]	[10^{-6}mol.m^{-2}]	[%]		

Formatted: Font: Bold

Formatted: Heading 2

Formatted: Font: (Default) Times New Roman

Formatted: Heading 3, Indent: First line: 0 cm

Formatted: Subscript

Formatted: Subscript

S5P training set	0.00	+0.02	1.4	45.68	0.87	9,634
S5P test set	-0.04	-1.30	1.68	56.38	0.79	1,071

Table 12. Performance of the machine learning predictions of NO_2 tropospheric columns over all European urban areas included in the dataset. The training set and test set includes January-May 2019 and randomly sampled (90% and 10%) over that period.

2.3.2. Results

Detailed scores of the performance of the gradient boosting regressor with respect to the real observations such as mean bias (MB), normalised mean bias (nMB), root-mean-square error (RMSE), normalised root-mean-square error (nRMSE) and the Pearson Correlation Coefficient (PCC) can be found in Table 12. In order to check obvious cases of overfitting (i.e. when the GBM model is fitting too closely the data used for training and are thus lacking generalization skills regarding new data), results are shown for both training and testing datasets. The statistics on both training set, and test set show similar results such as low bias, good correlation but significant RMSE. The statistical performance obtained on the training set indicates Results indicate that there is no clear sign of overfitting in the predictions. Since TROPOMI data are available only from mid-2018, the training set is relatively small. For this reason, the predictions are featuring significant RMSE values and will have a large random error. Such RMSE values stay however in the range of surface site air quality ML machine learning predictions as shown in Section 3 and Table 23. The low mean bias and high correlation values indicate that the main BAU NO_2 tropospheric column variability is represented without large systematic errors. Subtracting the BAU NO_2 simulated columns with the actual observed NO_2 columns during the lockdown period (from 16 March 2020 to 30 April 2020) gives us an estimate of the reductions on the NO_2 background levels over the urban areas considered in this study on the major European urban areas. Figure 5 provides an example of time series over Madrid that shows the behaviour of the GBM against the real observations for 2019 (the training period) and 2020 (the actual simulation period). In 2019, the GBM predictions follow the variations seen in the observations but do however show differences, either being above or under the observations. In 2020, a similar behaviour is observed until the lockdown date where the GBM prediction show consistently higher values than the observations but still following the same variations as the observations. This shows that the GBM predictions based on BAU predictors are performing realistically and account for BAU variations. This provides a method to assess the pollution changes due to lockdown restrictions using satellite data in more robust way than the "before-during" or "year-to-year" methods.

Formatted: Font: (Default) Times New Roman
Formatted: Heading 3, Indent: First line: 0 cm
Formatted: Indent: First line: 1.27 cm
Formatted: Font: Not Bold
Formatted: Font: Not Bold
Formatted: Font: Not Bold
Formatted: Font: Not Bold

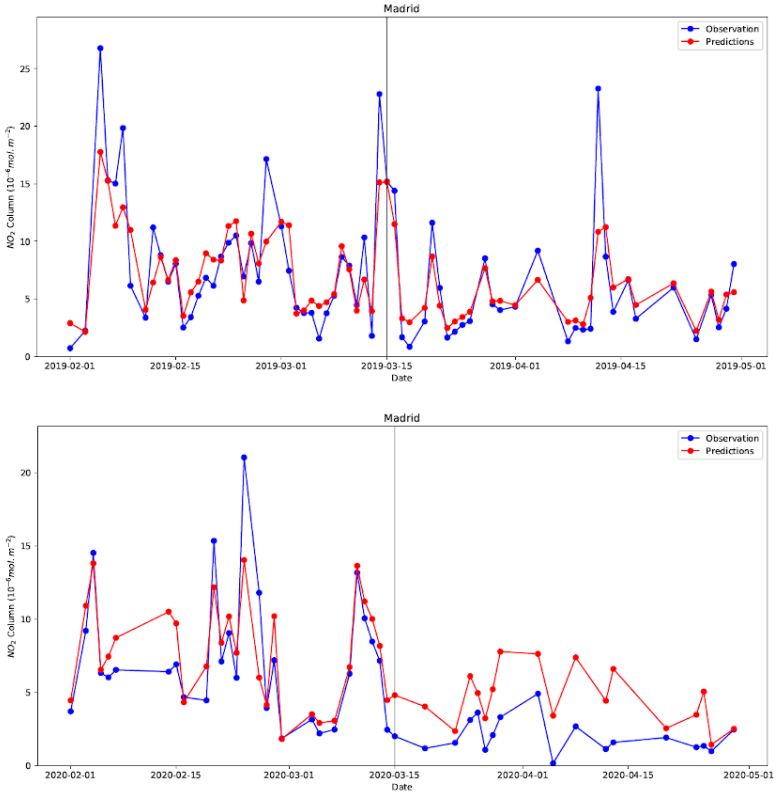

Figure 5. Example of time series over Madrid illustrating the performance of the machine learning NO_2 columns predictions for February-March-April 2019 (top panel) and 2020 (bottom panel).

Formatted: Font: Bold
Formatted: Font: Bold
Formatted: Centred, Indent: First line: 0 cm
Formatted: Font: Bold, Subscript
Formatted: Indent: First line: 0 cm

Figure 6~~5~~ shows the ML-based BAU equivalent estimates as in Fig. 3 and 4 for the pre-lockdown and lockdown periods. The estimates are based on the median value of the real observation minus simulated BAU observation distributions. As shown in table 1, the GBM performance shows large RMSE values and sometimes can generate strong differences due to the small training set used. We choose to display the median ~~and not the mean as the ML estimates~~ to as much as possible avoid the influence of potential ~~are generating strong~~ outliers in the estimates. ~~due to the small training set used.~~ The pre-

lockdowns ML estimates do not show as strong overall reductions as in the "year-to-year" (Fig. 4) or "before-during" (Fig. 3) estimates. A summary of the average and the standard deviation of the set of median estimates across all European urban areas considered is provided in Table 2 for each of the satellite methods. While both "year-to-year" and "before-during" methods showed substantial changes (24% and 30% respectively) of NO2 during the periods outside lockdown (i.e., in 2019 or before the lockdown in 2020) when low to no reduction should be expected, the ML-based weather-normalisation method provides changes closer to 0%, thus more realistic.

The weather-normalisation method is not devoid of uncertainties and can, in particular, be affected by trends on NO_2 levels. With a known trend seen in NO_x emissions of around 2 to 4% each year (EEA 2020a) and only one year to train the data, the ML method potentially estimates a stronger than expected overall reduction of around 8%. The "before-during" and the "year-to-year" approaches also show stronger reduction estimates on average during 2019 and the pre-lockdown period, respectively. Compared to the weather-normalisation approach, both methods also display a stronger standard deviation across cities than the weather-normalisation methods, which suggests substantial biases due to the omission of meteorological variability.

In the case of the lockdown period the weather parameter distributions are much more similar between 2019 and 2020 (Figure 2) and on average across Europe the "year-to-year" and weather-normalised estimates show results within in the same range in term of average (around -20%) and variability amongst the median estimates obtained in all urban areas (around 16%). This is however not the case for the "before-during" estimates which show much stronger variability between European urban areas (62%). The "before-during" estimates are then not reliable and the "year-to-year" is very dependent on the meteorological situation between 2019 and 2020. For this reason, the ML estimates are the most reliable and will be used solely for the rest of the study. Details of the ML estimates during the lockdown provided in Fig 6. are reported in the table in annex B. The NO_2 tropospheric column change estimates (median values per urban area) show on average a reduction of 23%, but urban areas that are known to have the most stringent measures (Hale et al., 2020) show much stronger reductions, e.g., Madrid 60%, Barcelona 59%, Turin 54%, Milan 49%. Lighter reductions can be observed in urban areas where less stringent measures were taken, e.g., Stockholm 17%. To check the robustness of such results, equivalent estimates are provided using surface stations and air quality models in section 3 and 4 and will be compared in section 5. ~~A summary of the results is provided in Table 3 displaying the average and the standard deviation of NO_2 changes across all European urban areas considered. The "before-during" and the "year-to-year" approaches also show stronger reduction estimates on average during 2019 and the pre-lockdown period, respectively. Such methods also display a stronger standard deviation across cities than the weather-normalization methods, which suggests substantial biases in the former due to the omission of meteorological variability.~~

Formatted: Subscript

Formatted: Indent: First line: 1.27 cm

Formatted: Subscript

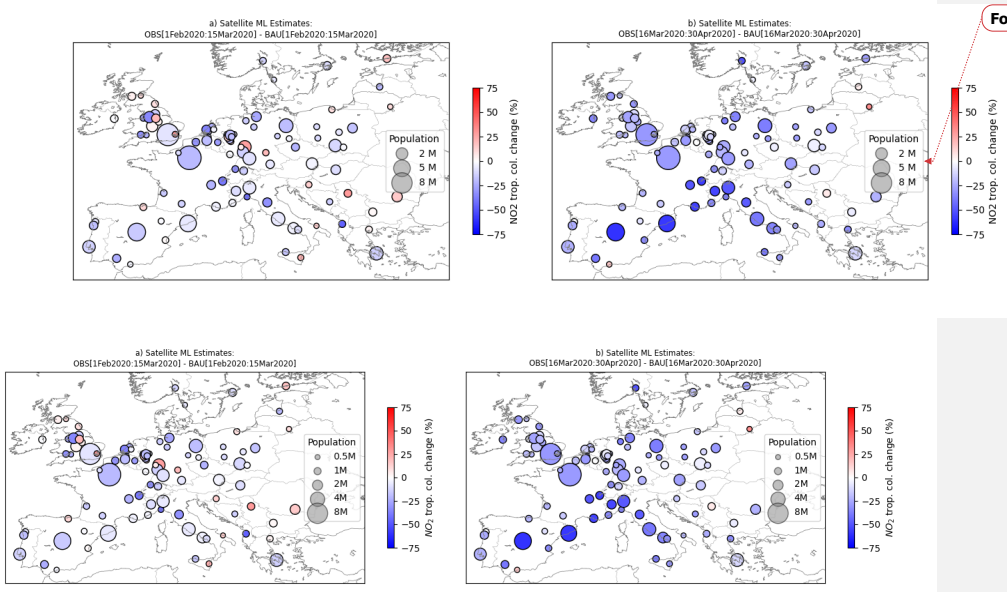

Figure 6~~5~~. TROPOMI-based estimation of tropospheric NO_2 column change (%, relative to the BAU predictions) for urban areas with at least 0.5 million inhabitants computed based on ML-based the weather-normalisation method for the pre-lockdown and lockdown periods (a and b respectively). The diameter of the circles is proportional to the population count in each urban area.

	Average (%)	Standard Deviation (%)
"Before-during" [2019]	-4034.45	4736.18
"Before-during" [2020]	-2530.20	6255.55
"Year-to-year" [01/02 to 15/03]	-2694.23	3128.42
"Year-to-year" [16/03 to 30/04]	-1821.78	16.36
Machine Learning [01/02 to 15/03]	-8.27	165.85
Machine Learning [16/03 to 30/04]	-232.72	165.51

Formatted: Justified, Indent: First line: 1.27 cm

Table 23. Scores over all European urban areas included in the dataset for the different TROPOMI NO_2 tropospheric columns change estimations. Average and standard deviation are calculated for all urban area resulting median estimates, i.e., the standard deviation is a metric of the inter urban area spread.

~~The weather-normalization method is not devoid of uncertainties. While a value close to zero would be expected during the pre-lockdown period, the method estimates a slight overall reduction of around -8%, partly due to the shortage of training data. It does however perform much better than the year-to-year and before-during methods that estimate a -24% and -30% reduction, respectively, during the pre-lockdown period. In the case of the lockdown period the weather parameter distributions are much more similar between 2019 and 2020 (Figure 2) and on average across Europe the "year-to-year" and weather-normalized estimates show results in the same range.~~

3. Surface station estimates

3.1. Methods

We have estimated the impact of the COVID-19 lockdown on surface NO_2 pollution in European areas using the methodology introduced by Petetin et al. (2020), applied to up to date (i.e., partly unvalidated real-time) hourly NO_2 data from the European Environmental Agency (EEA) AQ e-Reporting (EEA, 2020b). We first selected the urban/suburban background stations located within 0.1° from the city centres and applied the quality assurance and data availability screening described in Petetin et al. (2020), using the GHOST metadata (Globally Harmonised Observational Surface Treatment, Bowdalo et al., 2020, in preparation). A total of 164 stations in 77 urban areas were selected. At each station (independently), we estimated the BAU ~~business-as-usual~~ NO_2 mixing ratios that would have been observed during the lockdown period under an unchanged emission forcing. This was done using GBM models fed by meteorological inputs (2-m temperature, minimum and maximum 2-m temperature, surface wind speed, normalised 10-m zonal and meridian wind speed components, surface pressure, total cloud cover, surface net solar radiation, surface solar radiation downwards, downward UV radiation at the surface and PBL ~~boundary layer~~ height) taken from the 31km horizontal resolution ERA5 reanalysis dataset (Hersbach et al., 2020) in addition to other time features (date index, Julian date, weekday, hour of the day). ~~Using~~ T~~t~~he ERA5 reanalysis data set is~~has~~ a consistent model version over time but at coarser~~lower~~ resolution ~~(31km)~~ in comparison to the ECMWF high resolution ~~9km~~ operational forecasts used in the TROPOMI estimates (31 km versus 9 km).

All GBM models were trained and tuned during the past 3 years (2017-2019) and tested in 2020 before the lockdown. Petetin et al. (2020) showed that such a duration for training the GBM models is generally sufficient for capturing the influence of the weather variability on surface NO_2 mixing ratio. As discussed in more detail in Petetin et al. (2020), the date index feature here allows to limit the potential issues related to the presence of trends in the NO_2 time series (between 2% to 4%

Formatted: Centred
Formatted: Font: (Default) Times New Roman
Formatted: Heading 1, Indent: First line: 0 cm
Formatted: Font: (Default) Times New Roman, Font colour: Auto
Formatted: Heading 2, Indent: First line: 0 cm
Formatted: Indent: First line: 1.27 cm
Formatted: Font: Not Bold
Formatted: Font: Not Bold, Subscript
Formatted: Font: Not Bold
Formatted: Font: Not Bold, Subscript
Formatted: Font: Not Bold

decrease per year, EEA 2020a). If a substantial trend exists, the GBM models will put more importance on this feature, which in practice will force the model to make NO_2 mixing ratio predictions (in 2020) in the range of the values observed during the last part of the training dataset, ignoring the oldest training data. Thus, given the long-term reduction of NO_2 happening as a result of policy measures across Europe, considering longer training periods is not expected to improve the performance of the GBM models. ~~Using the last three years is long enough to capture weather variability at each site, but not too long with regards to long-term reduction of NO_2 happening as a result of policy measures across Europe.~~ In contrast, ~~Contrary to~~ Petetin et al. (2020) ~~that~~ predicted BAU NO_2 at the daily scale but, the ML models developed here are predicting NO_2 at the hourly scale (in order to get results collocated in time with TROPOMI overpasses, see below). We then deduced the weather-normalised NO_2 changes due to the lockdown by comparing observed and ML-based BAU NO_2 mixing ratios.

3.2. Results

Table 34 shows the overall performance of the GBM models on the training and test sets. Statistical results are similar to the TROPOMI NO_2 GBM model. Biases are low and correlation is high and there is a significant RMSE. As explained in section 2.3.2, s~~S~~tatistical scores in the training set and the test set suggest that there is no apparent sign of overfitting in the predictions and show reasonable performance. Note that the RMSE and PCC are deteriorated compared to the statistics obtained over Spain in Petetin et al. (2020), mainly due to the fact that we are here working at the hourly scale. This is demonstrated by the similar results as those of Petetin et al. (2020) that are obtained over this set of European cities when predicting NO_2 at the daily scale (for the test dataset: nRMSE=28%, PCC=0.88, N=11,082).

	MB [ppbv]	nMB [%]	RMSE [ppbv]	nRMSE [%]	PCC	N
Surface stations training set (2017-2019)	0.0	0.0	5.53	40.88	0.84	4,048,696
Surface stations test set (1 Jan 2020 – 15 Mar 2020)	+0.95	+7.02	6.24	45.87	0.80	268,960

Table 34. Performance of the ML ~~machine learning~~ predictions of hourly NO_2 surface mixing ratios over all European urban areas included in the dataset.

For a stricter comparison with the results discussed in Section 2., we provide two different estimates t~~T~~o account for ~~the potential error due to~~ the satellite sampling effect ~~we provide two estimates~~: either with complete hourly sampling or

Formatted: Font: Not Bold
Formatted: Font: Not Bold
Formatted: Font: Not Bold, Subscript
Formatted: Font: Not Bold
Formatted: Font: Not Bold, Subscript
Formatted: Font: Not Bold
Formatted: Subscript
Formatted: Font: (Default) Times New Roman, Font colour: Auto
Formatted: Heading 2, Indent: First line: 0 cm

filtered according to with S5P satellite overpass time (13:30 local solar time) and qa filtering (clear sky only) sampling. ~~for a stricter comparison with the results discussed in Section 2.~~ Figure 76 displays relative change estimates, showing the median of the distributions for each European city above 0.5 million inhabitants. ~~Overall~~Overall, the estimates for both samplings are broadly consistent, with ~~mean~~ NO_2 reductions~~changes~~ of around ~~-~~37% and ~~-~~43% on average for the hourly sampling and the S5P overpass sampling, respectively (Table 34). Such surface station estimates also show geographical variations similar to the satellite estimates, with larger reductions corresponding to locations with more stringent lockdowns (i.e., Spain, Italy and France) and less stringent lockdowns (i.e., Sweden, Germany). For example, Madrid shows reductions of 61% and 60% using the hourly surface stations and the satellite time sampled surface stations, which are very similar to the satellite estimates. On the opposite Stockholm show very slight reduction of 8% and 3% with the two different estimates. Such values are different from the satellites estimates (reduction of 17%) and pointing out some uncertainty regarding the estimates in this area.

Northern Europe (particularly Germany, Poland and the UK) displays larger NO_2 reductions with the estimates at satellite overpass time. This points out a possible dependence with the time of the day in the pollution and emission reductions. In general, those NO_2 relative changes based on surface in-situ concentrations are larger than the ones based on NO_2 tropospheric columns. Those two points are further discussed in section 5.~~This is expected as NO_2 surface site measurement do not directly translates to the TROPOMI NO_2 tropospheric column, which is the integrated NO_2 content from the surface to about the 200hPa altitude. Due to the short lifetime of NO_2, only marginal lockdown induced changes of free tropospheric NO_2 contents are expected. Changes are mainly expected near surface and within the PBL. Also, even if the stations are grouped within a 0.1° range from the city centres the representativeness of surface observations used might not be similar to a 0.1°x0.1° pixel, depending on the surface station coverage on each city. This can also exacerbate the difference between surface and tropospheric columns reduction estimates.~~

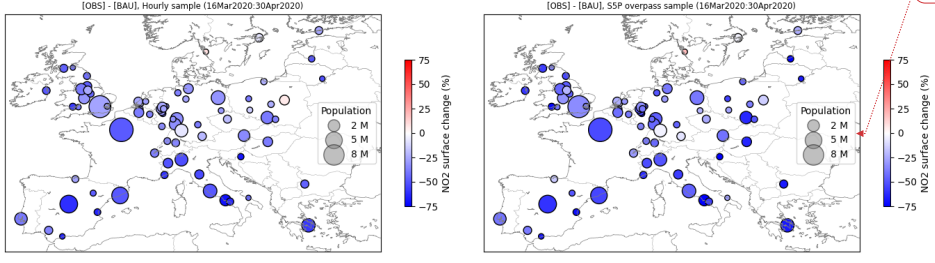

Formatted: Indent: First line: 1.27 cm

Formatted: Subscript

Formatted: Justified, Indent: First line: 1.27 cm

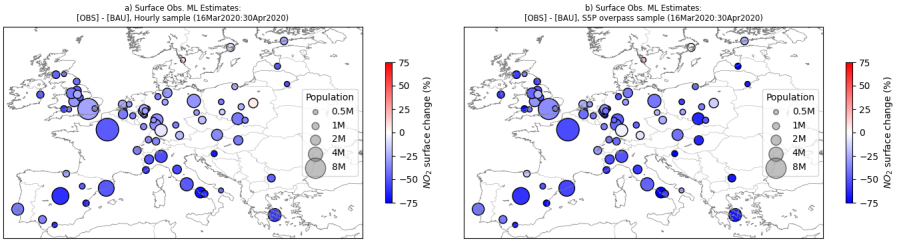

Figure 7~~6~~. ~~Surface observation~~ Weather normalised estimation of NO_2 changes (%, relative to the BAU predictions) using surface observations during the lockdown period using business as usual (BAU) simulated observations for urban areas with at least 0.5 million inhabitants. Left-hand side (a) are the estimates using full hourly datasets and right-hand side (b) are the estimates using S5P overpass time sampled dataset. The diameter of the circles is proportional to the population count in each urban area.

4. CAMS regional ensemble model estimates

4.1. Methods

Formatted: Heading 2

Model estimates have been calculated using the CAMS European regional air quality forecasting framework, which is an ensemble of 11 models (~~CHIMERE, DEHM, EMEP MSC-W, EURAD-IM, GEM-AQ, Lotos-Euros, MATCH, MINNI, MONARCH, MOCAGE, SILAM,~~ Marécal et al. 2015). These models are used to calculate multi-model median value which is the best performing quantity on average compared to individual models. Using such a multi-model approach is useful to minimize the imperfections in each model~~'s~~ formulation. Operational evaluation and validation of the CAMS European ensemble against independent observations is performed and delivered routinely and can be accessed at https://atmosphere.copernicus.eu/index.php/regional-services.

Two sets of models hindcasts have been conducted using two different emissions scenarios: BAU emissions and reduced COVID-19 lockdown emissions. The emission inventory used for the BAU reference simulation is the same that is used in the daily Regional Air Quality Forecasts of CAMS for Europe, i.e., CAMS-REG-AP (v3.1 for the reference year 2016, Granier et al., 2019). It is compiled by TNO (Netherlands Organisation for Applied Scientific Research) under the CAMS emission Service, based on official emissions reported by the countries to the EU (NEC Directive) and UNECE (LRTAP Convention /EMEP, ~~) (~~Kuenen et al., 2014~~; Granier et al., 2019~~). The spatial resolution of the emissions is 0.1° × ~~x~~0.05° but later re-gridded at 0.1° × ~~x~~0.1° to match the models' grid. The alternative emission scenario, corresponding to the lockdown

period, was derived by combining the original CAMS-REG-AP inventory with a set of country- and sector-resolved reduction factors (Guevara et al., 2020). For the present work, time invariant emission reduction factors ~~where~~were proposed by country and for three activity sectors: manufacturing industry, road transport, and aviation (landing and take-off cycles) that are reduced on average by 15.5%, 54% and 94%, respectively. These sectors were considered to be the most affected by changes in activity during lockdown (Le Quéré et al., 2020).

The reduction factors were computed from collections of near-real time activity data, such as Google Community Mobility Reports (Google LLC, 2020) for road transport, airport statistics from Flightradar24 (2020) for aviation and electricity load information from ENTSO-E (2020) for industry. Results from Guevara et al., (2020) showed that during the most severe lockdown period (23 March to 26 April), estimated surface emission reductions at the European level were most important for NO_x (33%) with road transport being the main contributor to total reductions in all cases (85% or more). Italy, France and Spain were the countries that experienced major NO_x emission reductions (down to 50%), a result that is in line with the strong lockdown restrictions implemented by their corresponding governments. On the contrary, Sweden, for example, showed reductions of only 15% (on NO_x) due to implementation of national recommendations instead of a state-enforced lockdown. More details about the emission scaling procedure using data and methodology from Guevara et al., 2020 can be found in Colette et al. (2020) where the resulting country and activity sector dependent reduction factors are provided for the EU28 countries plus Norway and Switzerland. Values of the emission reduction factors per country within the European regional modelling domain and per activity sectors and are provided in annex C. For the main contributing sector, road transport, the largest reductions in emissions are observed in countries where lockdown restrictions were more stringent (according to the Oxford Coronavirus Government Response Tracker stringency index Hale et al., (2020)), such as Italy (75%), Spain (80%) and France (76%).

~~The largest reductions are observed in those countries where lockdown restrictions were more stringent, such as Italy, Spain and France.~~ All the models operated with the exact same setup as the CAMS regional operational production. The modelling domain covers Europe at 0.1° × ~~x~~0.1° resolution. The meteorological and chemical boundary conditions are obtained from the Integrated Forecasting System (IFS) of ECMWF, which is the same system that provides part of the dataset for the ML-based estimations (see sections 2~~3.1~~ and 3~~2.2~~). The reference simulation was using the BAU anthropogenic emissions as described above and the lockdown scenario was using the same lockdown inventory, modulated by country and activity sectors. From the two sets of 11 model simulations the median at each grid point is calculated from an ensemble simulation (as is routinely done for the operational CAMS predictions, Marecal et al., 2015). Differences between the BAU ensemble and the lockdown scenarios ensemble are then used to calculate model reduction estimates.

4.2. Results

Figure 8~~7~~ displays the relative change estimates for each European urban area~~city~~ defined in section 2.2~~with more than half a million inhabitants~~. The estimates are ~~,~~ calculated using~~ing~~ the median~~s~~ of the full hourly distribution (Fig. 8~~7~~a)

Formatted: Font: 10 pt
Formatted: Font: 10 pt
Formatted: Font: 10 pt
Formatted: Font: 10 pt
Formatted: Font: 10 pt
Formatted: Subscript
Formatted: Font: 10 pt
Formatted: Font: (Default) +Body (Times New Roman), 10 pt
Formatted: Font: (Default) +Body (Times New Roman), 10 pt
Formatted: Font: (Default) +Body (Times New Roman), 10 pt, Subscript
Formatted: Font: (Default) +Body (Times New Roman), 10 pt
Formatted: Font: (Default) +Body (Times New Roman), 10 pt
Formatted: Font: (Default) +Body (Times New Roman), 10 pt
Formatted: Font: (Default) +Body (Times New Roman), 10 pt
Formatted: Font: (Default) +Body (Times New Roman), 10 pt
Formatted: Font: (Default) +Body (Times New Roman), 10 pt
Formatted: Font: (Default) +Body (Times New Roman), 10 pt
Formatted: Font: (Default) +Body (Times New Roman), 10 pt, Subscript
Formatted: Font: (Default) +Body (Times New Roman), 10 pt
Formatted: Font: (Default) Times New Roman
Formatted: Font: Bold
Formatted: Indent: First line: 0 cm

and of the distribution at qa filtered S5P overpasses times and dates only (Fig. 87b) at each urban area. As expected, urban areas in more stringentstricter lockdown countries (i.e., Spain, Italy, France) show the largest reductions (e.g., down to 60% in Madrid, see Figure 98) whereas urban areas with less stringent softer lockdown measures (i.e., Germany, Poland, Sweden) show milder reductions (e.g., around 16% in Stockholm, see Figure 8). The time sampling difference (hourly versus S5P overpass) does not affect the model estimates much, only few percent differences are seen for most of the European urban areas. On average, over the set of median estimates on each urban area the difference is small, with 30% for hourly estimates and 32% for S5P sampled estimates. This is expected as the emissions reduction estimates used to generate the lockdown scenario ensemble are set constant over time (daily and hourly). This point is further expanded in the next section where model estimates results are compared to the other types of estimates.~~. In comparison, the surface station estimates show more sensitivity to the time sampling. Table 4 summarises the overall European reduction estimates. On average, the S5P overpass sampling changes the estimates by around -6% for surface station estimates and -1.5% for model estimates. This could suggest a dependence between the time of day and the reduction level (e.g. traffic emissions are peaking daytime hence more reduction should be expected during the day). This topic needs to be further investigated.~~

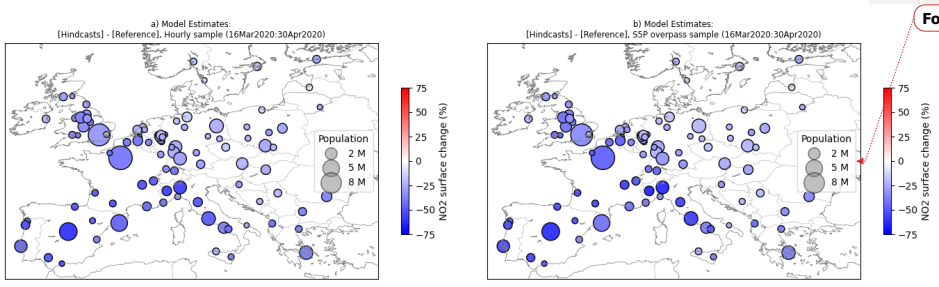

Formatted: Justified, Indent: First line: 1.27 cm

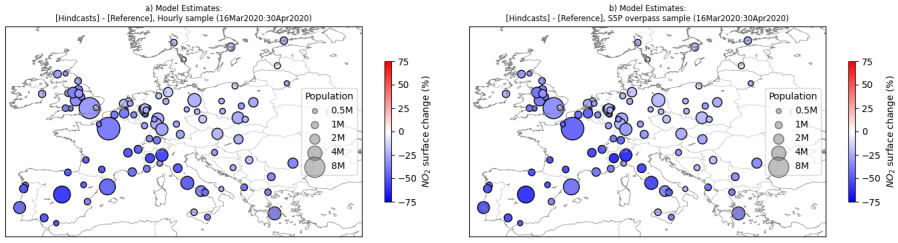

Figure 87. Surface modelling estimation of NO_2 changes (%, relative the BAU predictions) during the lockdown period in urban areas with at least 0.5 million inhabitants. Left-hand side (a) are the estimates using full hourly datasets and right-hand side (b) are the estimates using S5P overpass time sampled dataset. The diameter of the circles is proportional to the population count in each urban area.

	Average (%)	Standard Deviation (%)
Surface Stations [hourly]	-36.74	15.09
Surface Stations [S5P sampling]	-43.06	18.82
CAMS model ensemble [hourly]	-30.35	10.79
CAMS model ensemble [S5P sampling]	-31.82	11.97
TROPOMI	-22.72	15.51

Table 4. Scores over all European urban areas included in the study for the different NO2 changes estimates: surface stations, model estimates and TROPOMI. Average and standard deviation are calculated for all urban area resulting estimates, i.e. the standard deviation is a metric of the inter urban area spread.

5. Comparison of the three different types of estimates

In table 4 and figure 9 we summarize the results of this study. Table 4 shows the average reduction of all the median estimates with the inter urban area variability over Europe. Figure 9 shows the distribution of the NO_2 changes estimated along the lockdown period per urban area. This figure provides estimates equivalent to box plots where the median and the inter-quartile range are displayed. For clarity, we choose to display on Fig. 9 only urban areas that are above 1 million inhabitants. The values of each estimates for all urban area considered in this study are given in the table in annex B.

Formatted: Font: (Default) Times New Roman, Not Bold
Formatted: Heading 1, Left
Formatted: Font: (Default) Times New Roman
Formatted: Subscript

The three types of estimates agree on identifying stronger reductions where more severe lockdown measures were implemented. As shown in Section 2 satellite estimates show a relationship between NO_2 tropospheric columns reductions and the extent and generalization of restrictive measures in each country. A similar relationship is observed for surface sites and model estimates (Sections 3 and 4). The largest NO_2 reduction estimates of around 50% to 60% for both surface and tropospheric column are found in Spanish, Italian and French urban areas. In countries that implemented softer lockdown measures urban areas show lower reductions, e.g., Germany, Netherland, Poland or Sweden. Although significant discrepancies exist between the satellite, surface and model estimates in urban areas such as for example Naples (Italy), Sofia (Bulgaria), Katowice (Poland), the three methods provide overall a consistent broad picture. This is remarkable to note particularly as satellite data are concerned and this result contributes to establish their usefulness for urban air quality and not only for atmospheric pollution in general. Having a range of three different types of estimates help us to provide pollution changes across Europe with a certain level of certainty. When all the estimates agree it is more likely that the values of reduction due to the lockdown implementations are reliable. Conversely, if the different types of estimates show discrepancies not as much confidence should be given to the reduction values. In certain urban areas the estimates show certainty as they are close to each other. In Fig. 8, Madrid, Turin and Milan, to mention few urban areas, show consistency between the different type of estimates expressing more certain. In other locations such as Sofia, Athens and Budapest, strong discrepancies indicate that the estimates could be uncertain. Average scores on table 4 shows that surface stations provide stronger reduction estimates and satellite estimates provide weaker reduction estimates. Model estimates are laying mostly in between and showing much less spread within a given urban area (bars in Fig. 9) and less variations between urban areas (standard deviation in Table 4). The origin of such differences can be various and are detailed below.

Machine learning estimates that are observation based (satellite and surface stations) are showing more spread compared to the model estimates. In Fig 9. the inter-quartile ranges for the ML estimates are much larger than for the model estimates. A part of this difference in the spread is due to the variability representation. Machine learning observation-based estimates display more spread that includes a stronger variability than model estimates. Such large ranges show that there is a strong spread in the ML based estimates that is not seen in the model-based estimates. Model estimates are induced by emission country dependent reduction/scaling factors that are constant over time. In that case, the variability is induced by the changes in atmospheric conditions but not by changes in the emissions. The estimates from the ML approach can represent the transition into the lockdown where emission gradually decreased. This is contributing to the increased spread seen in the ML estimates. Scores from ML estimates (see table 1 and 3) also show significant RMSE that can add noise to the time series and then add to the resulting spread of the distributions. Stronger spread in TROPOMI estimates is likely due to the small training set used. Also, as time goes more TROPOMI data will be available to strengthen the reliability of the method. Disentangling the noise and the actual variability would need to be carefully done in further works.

All the different estimates presented in this study are consistent in scales using $0.1° \times 0.1°$ TROPOMI averaged pixels that match the CAMS forecasts and surface stations within a 0.1° range from the city centre. Some of the smaller urban areas considered in this study likely display a footprint that is finer than 0.1°, meaning that the urban pollution levels from the urban

Formatted: Indent: First line: 1.27 cm

area is mixed with low pollution background levels. This could cause the pollution changes in the gridded estimates to be weaker than expected in certain urban areas (e.g., Katowice, Budapest, Glasgow, etc.). Also, even if the urban/suburban background stations are selected, the in-situ surface observations sample the pollution levels within a 0.1° × 0.1° pixel given their location. This sampling might not be exactly representative of the average pollution footprint within the same pixel. This average is the information given by the models or the satellites. Such representativeness issues contribute to create discrepancies between the type of estimates and hence generate uncertainty. The differences seen in Fig. 9 between surface station estimates and gridded estimates (models and satellites) point out such possible representativeness issues. Representativeness is a difficult and important topic and deserves further research as it would require careful examination of the station's locations in specific urban areas and also using higher resolution modelling than 10 km.

Satellite overpass local times (13:30 local solar time) and presence of clouds in the measurement pixel can potentially influence the reduction estimates using TROPOMI data. We considered 1.5 months to compute the satellite reduction estimates. Overall, the sample size (S5P valid overpasses) in Fig. 9 ranges between 14 (Sevilla) and 37 (The Hague). On the same Fig. 9, surface sites and model estimates are displayed for hourly and S5P sampled estimates. Smaller or larger samples cannot really explain discrepancies between all the different estimates. Results however can be affected when the sample size becomes statistically very small and if shorter time periods (e.g., 1 or 2 weeks) are considered for satellite reduction estimates. Very small samples over the 6 weeks period were not considered in this study to avoid this effect. The effect of sampling also shows greater changes in the surface station estimates than in the model estimates. As mentioned above and seen in Fig 9. the surface station estimates provide more variability that account for hourly variations. The model estimates have fixed emission scaling factors for the entire lockdown period considered. The surface station estimates show more sensitivity to the time sampling than the model estimates. On average (see table 4), the S5P overpass sampling changes the estimates by around -6% for surface station estimates and only by -1.5% for model estimates. This suggest that the lockdown-induced reduction estimates depend upon the time of the day, i.e., when the road transport activity is peaking. The TROPOMI overpass time is 13:30 local solar time which is potentially an active time for road transport in many urban areas.

Finally, the tropospheric columns NO_2 reduction estimates displayed in Fig. 9 are generally not as strong as the NO_2 surface estimates (sites and model). Some exceptions can be seen in certain Spanish (e.g., Barcelona, Madrid) and Italian (e.g., Milan, Turin) urban areas where column estimates are close to the surface estimates, but overall column reductions are weaker. With all urban areas considered, the satellite estimates show around 23% reduction on average, which is 10% to 20% less than the model and surface station estimates (see table 4). This can be expected as NO_2 surface site measurements do not directly translate to the TROPOMI NO_2 tropospheric column, which is the integrated NO_2 content from the surface to about the 200hPa altitude. Due to the short lifetime of NO_2 (around 12 hours), only small lockdown induced changes to the free tropospheric NO_2 contents are expected. Changes are mainly expected near-surface and within the PBL. However, the different nature of the vertical sampling is likely to contribute to the differences between the relative reduction estimates from tropospheric columns versus surface concentrations. Further work will be needed to link quantitatively tropospheric columns and surface

Formatted: Font: Not Bold

levels variations, including sampling the model estimates using an observation operator commonly used in data assimilation and inverse modelling systems. This important work will be carried out in a further study.

	Average (%)	Standard Deviation (%)
Surface Stations [hourly]	-37	15
Surface Stations [S5P sampling]	-43	19
CAMS model ensemble [hourly]	-30	11
CAMS model ensemble [S5P sampling]	-32	12
TROPOMI	-23	16

Table 4. Scores over all European urban areas included in the study for the different NO_2 changes estimates: surface stations, model estimates and TROPOMI. Average and standard deviation are calculated for all urban area resulting estimates, i.e., the standard deviation is a metric of the inter urban area spread.

6. Conclusions

In this paper, we first show the importance of accounting for weather variability in satellite-based estimates of NO_2 changes due to the COVID-19 lockdown. While focusing over Europe and using the TROPOMI instrument, we show that the satellite estimates based on direct comparisons between different time periods without accounting for weather variability can be flawed and should not be used for this kind of assessment. To account for weather variability in satellite estimates, we use a recently developed methodology based on the gradient boosting machine learning technique. This methodology has proven to be efficient with surface sites to estimate lockdown induced changes over Spain (Petetin et al., 2020). We extended those surface estimates over Europe to compare with the satellite estimates. Finally, we included NO_2 changes estimates predicted by the 11 models CAMS regional ensemble, using emission reduction factors representative of the lockdown period. By providing and comparing the three different methodologies we provided a comprehensive and complementary assessment of NO_2 pollution level changes during the COVID-19 European lockdown. Providing such assessment of pollution changes when activity levels of keys emitting sectors are significantly reduced (i.e., road transport and industry) in lockdown conditions provides crucial information to accurately quantify the benefits of air quality policies implementations on such sectors.

Main results show a consistent tendency of stronger reduction of NO_2 where more stringent lockdown measures where implemented. On average the three types of estimates show a reduction of 23%, 43% and 30% for satellite, surface stations and model estimates, respectively. Differences are explained by the different nature the methods used, i.e., observation based versus model based, horizontal and vertical sampling, variability representation and time sampling. By providing an array of different methods we ensure that such pollution reduction estimates are reliable in certain urban areas and somewhat uncertain in others. Quantifying pollution changes accurately and insuring reliability is important for the impact on the COVID-19 pandemic itself as several studies have investigated the correlation between the high level of COVID-19 mortality and

Formatted: Subscript

atmospheric pollution (e.g., Contincini et al. 2020, Ogen et al. 2020, Achebak et al., 2020). Feedbacks are then to be expected between the effects of short-term air pollution exposure on COVID-19 mortality and lockdown measures. Beyond the quantification of the impact of COVID-19-related restrictions on pollutant concentrations, the observation-based weather-normalisation methodology used in this study is of general interest for assessing the impact of any type of emission changes (e.g., regulation and policy) on air quality (Grange et al., 2018, 2019) in the future.

Formatted: Font colour: Text 1, Pattern: Clear (White)

Formatted: Justified

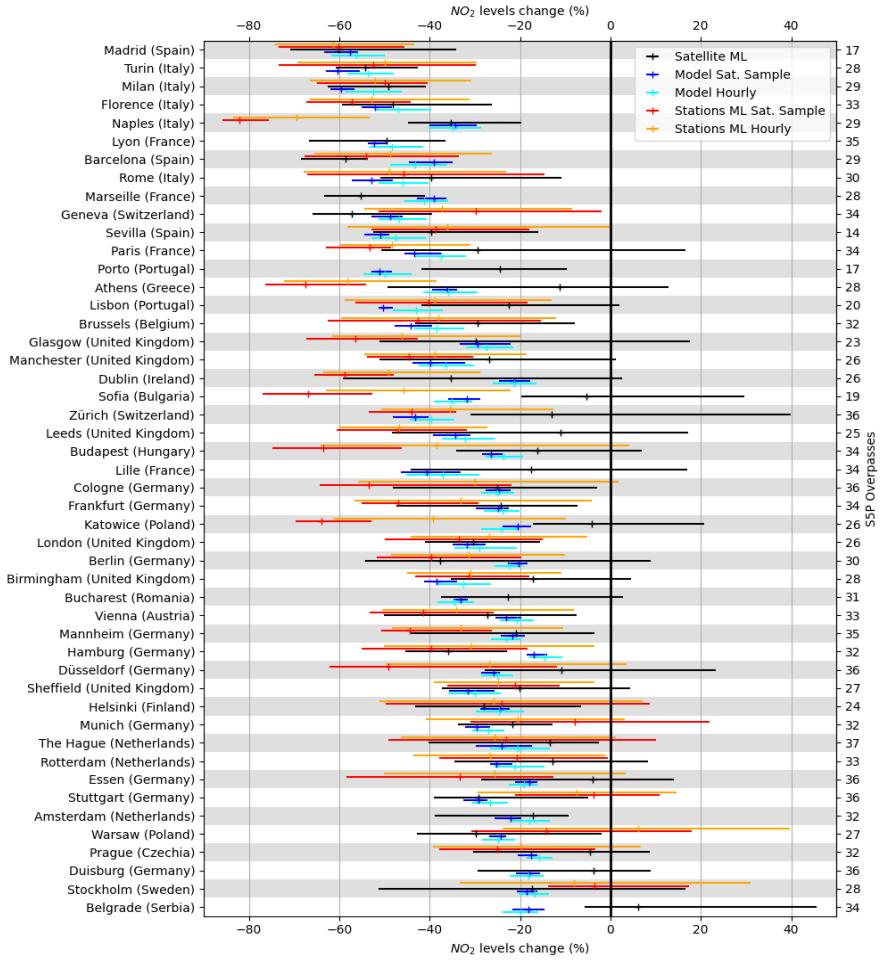

Figure 9. Comparisons of the lockdown induced NO_2 level changes estimates (%, relative to the BAU predictions) using different means and methodologies for European urban areas above 1 million inhabitants. Horizontal lines

represent the interquartile ranges (over the temporal variability), and the ticks are the median values using the full distribution per urban area. For readability, urban areas are ranked using the average between all median estimates.

~~Summary and Discussions~~

~~In this paper, we first show the importance of accounting for weather variability in satellite-based estimates of NO_2 changes due to the COVID-19 lockdown. While focusing over Europe and using the TROPOMI instrument, we show that the satellite estimates based on direct comparisons between different time periods without accounting for weather variability can be flawed and should not be used for this kind of assessments. To account for weather variability in satellite estimates, we use a recently developed methodology based on the gradient boosting machine learning technique. This methodology has proven to be efficient with surface sites to estimate lockdown induced changes over Spain (Petetin et al., 2020). We extended those surface estimates over Europe to compare with the satellite estimates. Finally, we included NO_2 changes estimates predicted by the 11 models CAMS regional ensemble, using emission reduction factors representative of the lockdown period. By providing and comparing the three different methodologies we provided a comprehensive and complementary assessment of NO_2 pollution level changes during the COVID-19 European lockdown. Providing such assessment is crucial to accurately quantify the lockdown pollution changes for air quality policy but also for the impact on the COVID-19 pandemic itself. Several studies have investigated the correlation between the high level of COVID-19 mortality and atmospheric pollution (e.g. Contincini et al. 2020, Ogen et al. 2020, Achebak et al., 2020). Feedbacks are then to be expected between the effects of short-term air pollution exposure on COVID-19 mortality and lockdown measures.~~

~~In Figure 8 and Table 4 we summarize the results of this study. While Table 4 shows the average reduction with the inter urban area variability over Europe, Figure 8 shows the difference between the estimates per urban area. For clarity and relevance, we choose to display only urban areas that are above 1 million inhabitants. The three weather normalized estimates agree on identifying stronger reductions where more severe lockdown measures were implemented. As shown in Section 2 satellite estimates show a relationship between NO_2 tropospheric columns reductions and the extent and generalization of restrictive measures in each country. A similar relationship is observed for surface sites and model estimates (Sections 3 and 4). The largest NO_2 reduction estimates of around 50% to 60% for both surface and tropospheric column are found for Spanish, Italian and French urban areas concentrations. In countries that adopted softer lockdown measures urban areas show lower reductions, e.g. Germany, Netherland, Poland or Sweden. Although significant discrepancies exist between the satellite, surface and model estimates in urban areas such as for example Naples (Italy), Sofia (Bulgaria), Katowice (Poland), the three methods provide overall a consistent broad picture. This is remarkable to note particularly as satellite data are concerned and this result contributes to establish their usefulness for urban air quality and not only for atmospheric pollution in general.~~

~~Machine learning observation-based estimates display more spread that includes a stronger variability than model estimates. In Figure 8, satellite and surface observation ML estimates show large interquartile ranges, with larger ranges with satellite for certain urban areas. Such large ranges show that there is a strong spread in the ML based estimates that is not seen~~

in the model-based estimates. Model estimates are induced by emission country dependent reduction/scaling factors that are constant over time. In that case variability is induced by the changes in atmospheric conditions but not by changes in the emissions. The estimates from the ML approach can represent the transition into the lockdown where emission gradually decreased. This is contributing to the increased spread seen in the ML estimates. Scores from ML estimates (see table 2 and 4) also show significant RMSE that can add noise to the time series and then add to the resulting spread of the distributions. Stronger spread in TROPOMI estimates are likely due to the small training set used. Also, as time goes more TROPOMI data will be available to strengthen the reliability of the method. Disentangling the noise and the actual variability would need to be carefully done in further works.

In all the different estimates presented above we tried to be consistent in scales using 0.1°x0.1° TROPOMI averaged pixels that match the CAMS forecasts and background stations within a 0.1° range from the city centre. Some urban areas considered in this study likely display a background footprint that is finer than 0.1°. The differences seen between surface station estimates and gridded estimates (models and satellites) point out such possible representativeness issues. Resolution representativeness is a difficult and important topic and deserves further research as it would require higher resolution modelling forecasts and an observation network at a resolution finer than 10km.

Satellite overpass local times and presence of clouds in the measurement pixel can potentially influence the reduction estimates using TROPOMI data. We considered 1.5 months to compute the satellite reduction estimates. Overall the sample size (S5P valid overpasses) in Figure 8 ranges between 14 (Sevilla) and 37 (The Hague). On the same Figure 8, surface sites and model estimates are displayed for hourly and S5P sampled estimates. Smaller or larger samples cannot explain discrepancies between all the different estimates. Results however can be affected when the sample size becomes statistically very small and if shorter time periods (e.g. 1 or 2 weeks) are considered for satellite reduction estimates. Very small samples were not considered in this study. Sampling also shows greater changes in the surface station estimates than in the model estimates. This can suggest that the lockdown-induced reduction estimates could also depend upon the time of the day. Further and more detailed research is needed on this topic.

Finally, tropospheric columns NO_2 reduction estimates are mostly smaller than the NO_2 surface estimates (sites and model). The different nature of the vertical sampling (tropospheric columns versus surface concentrations) affects the relative reduction estimates. Some exceptions can be seen in certain Spanish and Italian urban areas where column estimates are close to the surface estimates, but overall column reductions are weaker. Further work will be needed to link quantitatively tropospheric columns and surface levels variations. Including sampling the model estimates using an observation operator commonly used in data assimilation and inverse modelling systems. This important work will be carried out in a further study.

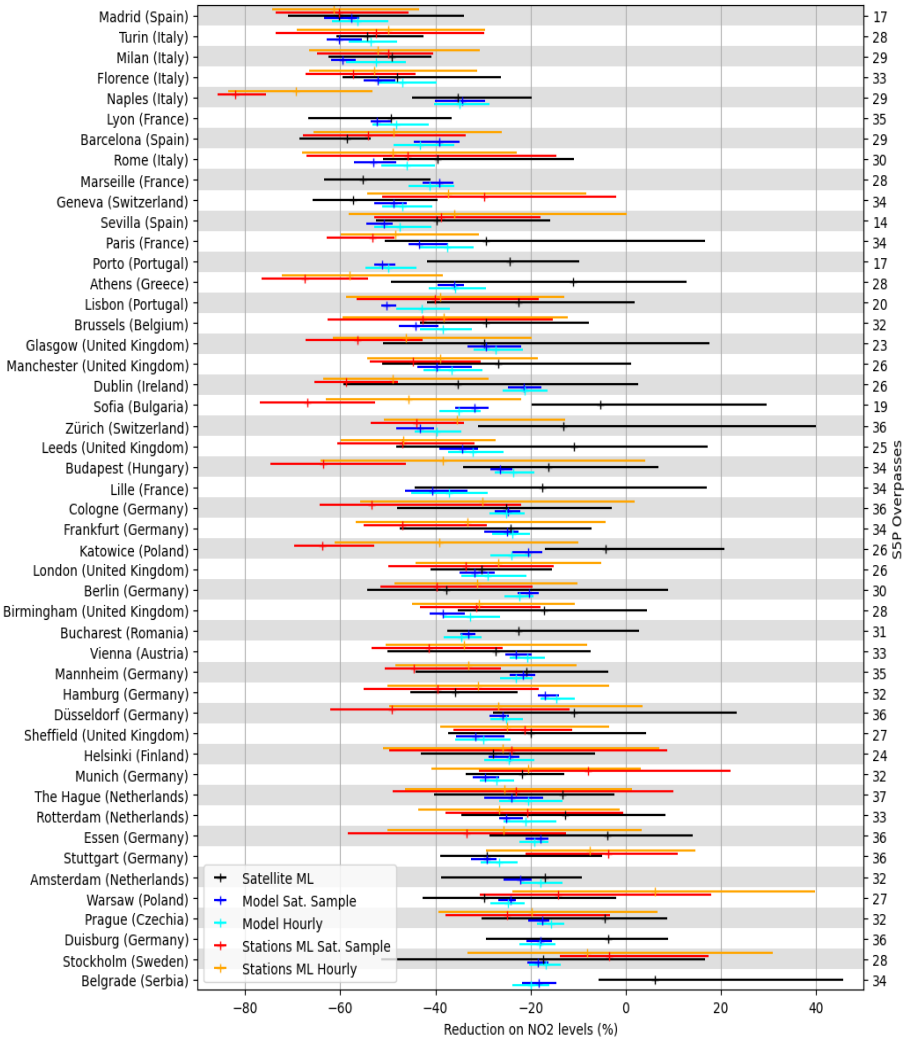
Madrid (Spain) 17
Turin (Italy) 28
Milan (Italy) 29
Florence (Italy) 33
Naples (Italy) 29
Lyon (France) 35
Barcelona (Spain) 29
Rome (Italy) 30
Marseille (France) 28
Geneva (Switzerland) 34
Sevilla (Spain) 14
Paris (France) 34
Porto (Portugal) 17
Athens (Greece) 28
Lisbon (Portugal) 20
Brussels (Belgium) 32
Glasgow (United Kingdom) 23
Manchester (United Kingdom) 26
Dublin (Ireland) 26
Sofia (Bulgaria) 19
Zürich (Switzerland) 36
Leeds (United Kingdom) 25
Budapest (Hungary) 34
Lille (France) 34
Cologne (Germany) 36
Frankfurt (Germany) 34
Katowice (Poland) 26
London (United Kingdom) 26
Berlin (Germany) 30
Birmingham (United Kingdom) 28
Bucharest (Romania) 31
Vienna (Austria) 33
Mannheim (Germany) 35
Hamburg (Germany) 32
Düsseldorf (Germany) 36
Sheffield (United Kingdom) 27
Helsinki (Finland) 24
Munich (Germany) 32
The Hague (Netherlands) 37
Rotterdam (Netherlands) 33
Essen (Germany) 36
Stuttgart (Germany) 36
Amsterdam (Netherlands) 32
Warsaw (Poland) 27
Prague (Czechia) 32
Duisburg (Germany) 36
Stockholm (Sweden) 28
Belgrade (Serbia) 34
S5P Overpasses
Satellite ML
Model Sat. Sample
Model Hourly
Stations ML Sat. Sample
Stations ML Hourly
−80
−60
−40
−20
0
20
40
Reduction on NO2 levels (%)

~~**Figure 8. Comparisons of the lockdown induced NO_2 level changes estimates (%) using different means and methodologies for European urban areas above 1 million inhabitants. Horizontal lines represent the interquartile ranges and the ticks are the median values using the full distribution per urban area. For readability, urban areas are ranked using the average between the all median estimates.**~~

Acknowledgements

The research leading to these results has received funding from the Copernicus Atmosphere Monitoring Service (CAMS), which is implemented by the European Centre for Medium-Range Weather Forecasts (ECMWF) on behalf of the European Commission. We acknowledge support from the Ministerio de Ciencia, Innovación y Universidades (MICINN) as part of the BROWNING project RTI2018-099894-B-I00 and NUTRIENT project CGL2017-88911-R, the AXA Research Fund and the European Research Council (grant no. 773051, FRAGMENT). We also acknowledge PRACE and RES for awarding access to Marenostrum4 based in Spain at the Barcelona Supercomputing Center through the eFRAGMENT2 and AECT-2020-1- 0007 projects. This project has also received funding from the European Union's Horizon 2020 research and innovation programme under the Marie Sklodowska-Curie grant agreement H2020-MSCA-COFUND-2016-754433. Carlos Pérez GarcíaPando also acknowledges support received through the Ramón y Cajal programme (grant RYC-2015-18690) of the MICINN. ~~This project has received funding from the European Union's Horizon 2020 research and innovation programme under the Marie Sklodowska-Curie grant agreement H2020-MSCA-COFUND-2016-754433.~~ Modelling and satellite data were produced by the *Copernicus Atmosphere Monitoring Service.* We thank the 3 anonymous reviewers for their helpful comments that improved this paper.

Annex A. Gradient Boosting Regressor Tuning

We have used TROPOMI data from 2019-01-01 to 2019-05-31 to train our machine learning simulator. We used the gradient boosting regressor function included in the scikit-learn python library. For validation purposes, the data set has been split between a training set (90% of the total dataset) and a test set (10% of the total dataset) using the train_test_split function. The hyperparameter tuning is then performed using the training set to generate the simulators and test set to find the best fit. Similarly, to Petetin et al. (2020) the learning rate was fixed to 0.05 and the number of features (max_features) is set to "sqrt". In addition, the tuning of the gradient boosting regressor was done for the following hyperparameters using the grid search method. The following hyperparameters were tuned: the subsample (~~subsample :~~subsample: from 0.3 to 1.0 by 0.1 with a best

Formatted: Heading 2

Formatted: Heading 2

value of 0.9), the number of trees (n_estimators: from 50 to 1000 by 50 with a best value of 400) and the minimum sample in terminal leaves (min_samples_leaf~~.~~: from 1 to 30 with a best value of 22). We use the default 5-fold cross-validation. We then test the final results on the test set in order ensure not overfitting.

Links to the python libraries and functions:
Scikit-learn python
https://scikit-learn.org/stable/index.html
Gradient boosting function
https://scikit-learn.org/stable/modules/generated/sklearn.ensemble.GradientBoostingRegressor.html
Grid search hyperparameter tuning
https://scikit-learn.org/stable/modules/generated/sklearn.model_selection.GridSearchCV.html
Random dataset splitting
https://scikit-learn.org/stable/modules/generated/sklearn.model_selection.train_test_split.html

Annex B~~B~~. Lockdown induced NO_2 changes estimates for each European urban area considered in this study

Urban Area	Country	TROPOMI Estimates (%)	N Revisits	Model Estimates Hourly (%)	Model Estimates S5P Sampled (%)	Surface Station Estimates Hourly (%)	Surface Station Estimates S5P Sampled (%)
Amsterdam	Netherlands	-17.08	32	-17.93	-22.12		
Antwerp	Belgium	-23.04	36	-21.13	-24.98	-32.79	-30.28
Athens	Greece	-11.13	28	-35.83	-36.06	-58.11	-67.5
Barcelona	Spain	-58.53	29	-43.23	-39.10	-48.81	-54.09
Bari	Italy	-20.13	33	-21.17	-18.29	-44.04	-27.54
Basel	Switzerland	-32.58	37	-31.49	-38.33	-32.95	-38.78
Belgrade	Serbia	6.05	34	-19.86	-18.20		
Berlin	Germany	-37.71	30	-22.27	-20.29	-31.28	-39.73
Bilbao	Spain	-21.29	19	-48.39	-50.45	-26.65	-15.36
Birmingham	UK	-17.24	28	-32.62	-38.41	-30.92	-31.38
Bonn	Germany	-4.55	35	-26.55	-29.04	-38.96	-61.62
Bordeaux	France	-21.59	28	-46.87	-50.39		

Bradford	UK	-24.36	26	-31.31	-33.66		
Braga	Portugal	-1.05	16	-42.93	-42.65		
Bremen	Germany	-37.36	34	-17.99	-19.56	-36.62	-49.47
Brighton	UK	-22.21	31	-20.55	-23.51	-22.75	-27.09
Bristol	UK	-19.47	30	-39.62	-43.63	-38.45	-38.54
Brussels	Belgium	-29.32	32	-38.38	-44.20	-38.16	-42.67
Bucharest	Romania	-22.58	31	-34.50	-33.11		
Budapest	Hungary	-16.18	34	-23.70	-26.36	-38.49	-63.53
Bytom	Poland	-11.97	30	-25.22	-22.21		
Caerdydd	UK	-18.76	31	-35.60	-41.59	-57.81	-72.57
Catania	Italy	-30.34	26	-35.08	-34.75		
Cologne	Germany	-25.04	36	-25.11	-24.74	-30.07	-53.41
Dortmund	Germany	-10.67	36	-23.84	-23.65	-28.63	-48.38
Dresden	Germany	-28.23	32	-21.82	-20.01	-29.26	-21.35
Dublin	Ireland	-35.36	26	-21.27	-21.34	-49.05	-58.8
Duisburg	Germany	-3.73	36	-18.18	-17.91		
Düsseldorf	Germany	-10.86	36	-25.13	-25.92	-26.82	-49.19
Edinburgh	UK	-16.29	23	-27.72	-28.01	-38.95	-34.01
Essen	Germany	-3.92	36	-19.18	-17.85	-25.68	-33.37
Florence	Italy	-48.04	33	-46.88	-52.11	-52.79	-57.22
Frankfurt	Germany	-24.24	34	-23.82	-24.94	-33.22	-46.9
Gdańsk	Poland	-16.67	30	-10.72	-10.09	-23.07	-43.45
Geneva	Switzerland	-57.27	34	-46.85	-48.78	-37.27	-29.81
Genoa	Italy	-35.81	30	-27.19	-26.87		
Glasgow	UK	-29.81	23	-27.33	-29.33	-46.12	-56.41
Gliwice	Poland	-23.30	32	-26.84	-25.04		
Göteborg	Sweden	-4.54	32	-10.18	-13.78	8.84	19.34
Hamburg	Germany	-35.87	32	-14.66	-17.05	-31.01	-39.61
Hannover	Germany	-19.02	33	-23.89	-24.86	-26.09	-29.14
Helsinki	Finland	-27.91	24	-24.63	-24.38	-25.81	-23.97
Katowice	Poland	-4.21	26	-24.03	-20.46	-39.22	-63.85
Kraków	Poland	-11.70	30	-21.07	-20.98	-36.88	-49.36
Leeds	UK	-10.98	25	-32.24	-34.30	-46.82	-47
Leipzig	Germany	-22.63	36	-22.42	-22.65		
Lille	France	-17.46	34	-37.14	-40.67		
Lisbon	Portugal	-22.48	20	-42.92	-50.26	-38.9	-40.18
Liverpool	UK	-3.72	29	-27.72			
Liège	Belgium	-0.44	34	-34.26	-34.95	-37.12	-39.66
Łódź	Poland	-11.58	30	-29.03	-28.65	-23.69	-37.71

London	UK	-30.38	26	-29.02	-31.73	-26.74	-33.58
Lyon	France	-49.43	35	-48.24	-52.33		
Madrid	Spain	-60.18	17	-56.28	-57.69	-61.38	-60.22
Manchester	UK	-26.72	26	-36.51	-39.78	-38.94	-44.68
Mannheim	Germany	-20.89	35	-23.09	-21.60	-33.04	-44.45
Marseille	France	-55.24	28	-41.24	-39.14		
Milan	Italy	-49.13	29	-52.53	-59.50	-52.08	-49.89
Munich	Germany	-21.72	32	-27.08	-29.57	-20.57	-7.93
Málaga	Spain	15.66	6	-50.30	-47.59	-63.08	-66.36
Naples	Italy	-35.28	29	-34.91	-34.39	-69.36	-82
Newcastle	UK	-30.01	22	-27.23	-30.15	-41.78	-53.53
Nice	France	-33.82	24	-38.02	-36.72	-59.47	-60.87
Nottingham	UK	-23.64	23	-34.84	-36.90	-44.84	-46.56
Nuremberg	Germany	-6.95	31	-27.47	-28.10	-38.62	-45.64
Oslo	Norway	-50.93	22	-20.18	-23.63		
Palermo	Italy	-38.72	26	-21.97	-22.73		
Paris	France	-29.37	34	-37.57	-43.43	-48.33	-53.28
Porto	Portugal	-24.41	17	-49.84	-51.19		
Poznań	Poland	-26.43	31	-21.90	-22.05	-38.38	-55.64
Prague	Czechia	-4.47	32	-15.75	-17.60	-19.74	-24.99
Riga	Latvia	5.06	30	-6.84	-7.27	-50.5	-84.04
Rome	Italy	-39.55	30	-46.04	-52.95	-49	-45.74
Rotterdam	Netherlands	-12.73	33	-21.09	-25.21	-26.62	-20.71
Rouen	France	-23.40	35	-39.66	-45.61		
Saarbrücken	Germany	-24.24	38	-27.59	-26.57	-33.47	-37.49
Salerno	Italy	-32.12	26	-42.88	-48.36	-61.57	-56.63
Sarajevo	Bosnia Herz.	-28.87	26	-22.54	-20.07		
Sevilla	Spain	-39.64	14	-47.55	-50.90	-36.1	-38.74
Sheffield	UK	-20.04	27	-29.98	-31.58	-24.87	-21.18
Sofia	Bulgaria	-5.34	19	-35.06	-31.85	-45.72	-66.84
Southend	UK	-26.99	29	-11.26	-11.11	-29.57	-37.41
Stockholm	Sweden	-17.44	28	-16.72	-18.45	-8.11	-3.46
Stuttgart	Germany	-29.26	36	-26.69	-29.23	-7.49	-3.73
The Hague	Netherlands	-13.33	37	-20.57	-24.07	-25.54	-23.09
Thessaloníki	Greece	-32.37	27	-35.97	-35.93		
Tirana	Albania	-24.05	26	-40.06	-40.78		
Toulouse	France	-15.56	24	-47.92	-50.72		
Turin	Italy	-54.29	28	-53.57	-60.29	-49.94	-52.44
Utrecht	Netherlands	-20.40	33	-25.45	-29.52	-28.38	-30.9

Valencia	Spain	-33.54	22	-34.71	-32.98	-63.35	-70.83
Vienna	Austria	-27.27	33	-20.78	-23.04	-34.07	-41.45
Vilnius	Lithuania	32.66	26	-25.18	-23.92	-50.6	-66.15
Warsaw	Poland	-29.68	27	-24.83	-24.20	6.19	-14.19
Wiesbaden	Germany	-26.34	33	-30.11	-31.35	-31.2	-43.57
Wrocław	Poland	-27.53	34	-22.51	-21.09	-14.16	-26.8
Wuppertal	Germany	-12.55	36	-24.56	-24.86	-27.35	-39.35
Zagreb	Croatia	-15.52	32	-28.65	-29.98	-68.09	-81.39
Zaragoza	Spain	-8.44	27	-44.85	-48.94	-47.12	-49.4
Zürich	Switzerland	-13.09	36	-39.70	-43.27	-35.41	-43.96

Annex C. Reduction factors (%) by country and activity sector corresponding to the lockdown period over the modelled European domain

Country	GNFR_B_Industry	GNFR_F_RoadTransport	GNFR_H_Aviation
Albania	-11,5	-77	
Austria		-54	-96
Belarus		-19	
Belgium	-11,0	-63	-96
Bosnia & Herz.		-43	
Bulgaria	-14,0	-48	-96
Croatia	-21,5	-65	-93
Czechia	-14,7	-41	-99
Germany	-11,5	-42	-87
Denmark	-17,3	-40	-97
Estonia	-15,2	-37	-92
Finland	-5,9	-53	-91
France	-29,0	-76	-94
Georgia		-75	
Great Britain	-21,0	-67	-88
Greece	-14,9	-66	-91
Hungary	-12,8	-50	-95
Ireland	-12,6	-64	
Italy	-18,9	-75	-93
Latvia	-12,7	-35	-99
Lithuania	-13,4	-47	-100

Formatted: Font: 10 pt

Formatted Table

Formatted: Font: 10 pt

Luxembourg	-11,2	-62	-86	Formatted: Font: 10 pt
Macedonia	-30,5	-49	-100	Formatted: Font: 10 pt
Malta		-48		Formatted: Font: 10 pt
Moldova	-21,5	-57		Formatted: Font: 10 pt
Netherlands	-27,1	-56	-91	Formatted: Font: 10 pt
Norway	-10,9	-38	-83	Formatted: Font: 10 pt
Poland	-12,3	-53		Formatted: Font: 10 pt
Portugal	-14,6	-73		Formatted: Font: 10 pt
Romania	-10,2	-62	-100	Formatted: Font: 10 pt
Russia		-38		Formatted: Font: 10 pt
Serbia		-57		Formatted: Font: 10 pt
Slovakia	-11,8	-51	-100	Formatted: Font: 10 pt
Slovenia	-10,7	-50	-91	Formatted: Font: 10 pt
Spain	-19,3	-80	-97	Formatted: Font: 10 pt
Sweden	-12,4	-31	-95	Formatted: Font: 10 pt
Switzerland		-47	-95	Formatted: Font: 10 pt
Turkey		-87		Formatted: Font: 10 pt
Ukraine		-23		Formatted: Font: 10 pt
AVG (+other)	-15,5	-54	-94	Formatted: Font: 10 pt

770

References

Arya P.S. Air Pollution Meteorology and Dispersion, Oxford University Press, New York (1999)

Barré, J., D. Edwards, H. Worden, A. Da Silva, W. Lahoz: On the feasibility of monitoring Carbon Monoxide in the lower troposphere from a constellation of Northern Hemisphere geostationary satellites. (Part 1), Atmospheric Environment doi:10.1016/j.atmosenv.2015.04.069, 2015

Bowdalo, D.: Globally Harmonised Observational Surface Treatment: Database of global surface gas observations, in preparation.

Bauwens, M. S. Compernolle, T. Stavrakou, J.-F. Müller, J. van Gent, H. Eskes, P. F. Levelt, R. van der A, J. P. Veefkind, J. Vlietinck, H. Yu, C. Zehner: Impact of coronavirus outbreak on NO_2 pollution assessed using TROPOMI and OMI observations. Geophysical Research Letters, https://doi.org/10.1029/2020GL087978, 2020.

Carslaw, D.C. and P.J. Taylor (2009). Analysis of air pollution data at a mixed source location using boosted regression trees. Atmospheric Environment. Vol. 43, pp. 3563–3570.

Colette, A., M. Schulz, M. Guevara, B. Raux, A. Mortier, S. Tsyro, F. Meleux, F. Couvidat, C. Geels, M. Gauss, E. Friese, J.W. Kaminski, J. Douros, R. Timmermans, R. Lennart, M. Adani, O. Jorba, R. Kouznetsov, M. Joly, A. Benedictow, H. Fagerli, L. Tarrason, P. Hamer and L. Rouïl, COVID impact on air quality in Europe, A preliminary regional model analysis, CAMS Policy Service Report, 2020, https://policy.atmosphere.copernicus.eu/reports/CAMS71_COVID_20200626_v1.3.pdf

Collivignarelli, M. C., A. Abba, G. Bertanza, R. Pedrazzani, P. Ricciardi, and M. C. Miino: Lockdown for CoViD-2019 in Milan: What are the effects on air quality? Science of the Total Environment, 732 (139280), https://doi.org/10.1016/j.scitotenv.2020.139280, 2020.

Contincini E., B. Frediani, and D. Caro: Can atmospheric pollution be considered a co-factor in extremely high level of SARS-CoV-2 lethality in Northern Italy? Environmental Pollution, 261, 114465, https://doi.org/10.1016/j.envpol.2020.114465, 2020.

EEA: European Union emission inventory report 1990-2018 under the UNECE Convention on Long-range Transboundary Air Pollution (LRTAP), EEA Report No 05/2020, 2020a.

EEA: Air Quality e-Reporting Database, European Environment Agency (http://www.eea.europa.eu/data- and-maps/data/aqereporting-8) 2020b.

ENTSO-E: Transparency Platform. Available at: https://transparency.entsoe.eu/ (last accessed, May 2020), 2020.

Eskes, H. et al., S5P Mission Performance Centre Nitrogen Dioxide [L2__NO2___] Readme, ESA, 01.03.02. https://sentinel.esa.int/documents/247904/3541451/Sentinel-5P-Nitrogen-Dioxide-Level-2-Product-Readme-File

Flightradar24. Airport statistics. Available at: https://www.flightradar24.com/data/airports (last accessed, May 2020), 2020.

Formatted: Font colour: Text 1

Formatted: Font: (Default) +Body (Times New Roman), 10 pt, Font colour: Text 1

Formatted: Line spacing: 1.5 lines

Friedman, J. H.: Greedy function approximation: A gradient boosting machine., The Annals of Statistics, 29, 1189–1232, https://doi.org/10.1214/aos/1013203451, http://projecteuclid.org/euclid.aos/1013203451, 2001.

Goldberg, D. L., Anenberg, S. C., Griffin, D., McLinden, C. A., Lu, Z., & Streets, D. G. (2020). Disentangling the impact of the COVID-19 lockdowns on urban NO_2 from natural variability. Geophysical Research Letters, 47, e2020GL089269. https://doi.org/10.1029/2020GL089269

Grange, S. K. and Carslaw, D. C.: Using meteorological normalisation to detect interventions in air quality time series, Science of The Total Environment, 653, 578–588, https://doi.org/10.1016/j.scitotenv.2018.10.344, 2019.

Grange, S. K., Carslaw, D. C., Lewis, A. C., Boleti, E., and Hueglin, C.: Random forest meteorological normalisation models for Swiss PM10 trend analysis, Atmospheric Chemistry and Physics, 18, 6223–6239, https://doi.org/10.5194/acp-18-6223-2018, https://www.atmos-chem-phys.net/18/6223/2018/, 2018.

Granier, C., Darras, S., Denier van der Gon, H. A. C., Doubalova,J., Elguindi, N., Galle, B., Gauss, M., Guevara, M., Jalkanen, J.-P., Kuenen, J., Liousse, C., Quack, B., Simpson, D., and Sindelarova, K.: The Copernicus Atmosphere Monitoring Service global and regional emissions (April 2019 version), Copernicus Atmosphere Monitoring Service (CAMS) report, 2019, https://doi.org/10.24380/d0bn-kx16, 2019

Google LLC. Google COVID-19 Community Mobility Reports. Available at: https://www.google.com/covid19/mobility/ (last access: May 2020), 2020

Guevara, M., Jorba, O., Soret, A., Petetin, H., Bowdalo, D., Serradell, K., Tena, C., Denier van der Gon, H., Kuenen, J., Peuch, V.-H., and Pérez García-Pando, C.: Time-resolved emission reductions for atmospheric chemistry modelling in Europe during the COVID-19 lockdowns, Atmos. Chem. Phys. Discuss., https://doi.org/10.5194/acp-2020-686, in review, 2020.

Hale, Thomas, Sam Webster, Anna Petherick, Toby Phillips, and Beatriz Kira (2020). Oxford COVID-19 Government Response Tracker, Blavatnik School of Government. Data use policy: Creative Commons Attribution CC BY standard.

Hersbach, H., Bell, B., Berrisford, P., Hirahara, S., Horanyi, A., Munoz-Sabater, J., Nicolas, J., Peubey, C., Radu, R., Schepers, D., Simmons, A., Soci, C., Abdallaa, S., Abellan, X., Balsamo, G., Bechtold, P., Biavati, G., Bidlot, J., Bonavita, M., De Chiara, G., Dahlgren, P., Dee, D., Diamantakis, M., Dragani, R., Flemming, J., Forbes, R., Fuentes, M., Geer, A., Haimberger,

Formatted: Font: (Default) +Body (Times New Roman), 10 pt, Font colour: Text 1

Formatted: Pattern: Clear

Formatted: Left

L., Healy, S., Hogan, R.J., Holm, E., Janiskova, M., Keeley, S., Laloyaux, P., Lopez, P., Radnoti, G., de Rosnay, P., Rozum, I., Vamborg, F., Villaume, S., Thepaut, J.N. (2020), The ERA5 Global Reanalysis, Quarterly Journal of the Royal Meteorological Society, https://rmets.onlinelibrary.wiley.com/doi/abs/10.1002/qj.3803

Kuenen, J. J. P., Visschedijk, A. J. H., Jozwicka, M., and Denier van der Gon, H. A. C.: TNO-MACC_II emission inventory; a multi-year (2003–2009) consistent high-resolution European emission inventory for air quality modelling, Atmos. Chem. Phys., 14, 10963–10976, https://doi.org/10.5194/acp-14-10963-2014, 2014

Ogen, Y: Assessing nitrogen dioxide (NO_2) levels as a contributing factor to coronavirus (COVID-19) fatality. Science of the Total Environment, 72 (138605), https://doi.org/10.1016/j.scitotenv.2020.138605, 2020.

Iolanda Ialongo, Henrik Virta, Henk Eskes, Jari Hovila, and John Douros, Comparison of TROPOMI/Sentinel-5 Precursor NO_2 observations with ground-based measurements in Helsinki, Atmos. Meas. Tech., 13, 205–218, https://doi.org/10.5194/amt-13-205-2020, 2020

Keller, C. A., Evans, M. J., Knowland, K. E., Hasenkopf, C. A., Modekurty, S., Lucchesi, R. A., Oda, T., Franca, B. B., Mandarino, F. C., Díaz Suárez, M. V., Ryan, R. G., Fakes, L. H., and Pawson, S.: Global Impact of COVID-19 Restrictions on the Surface Concentrations of Nitrogen Dioxide and Ozone, Atmos. Chem. Phys. Discuss. [preprint], https://doi.org/10.5194/acp-2020-685, in review, 2020.

Le, Tianhao, Yuan Wang, Lang Liu, Jiani Yang, Yuk L. Yung, Guohui Li, John H. Seinfeld, Unexpected air pollution with marked emission reductions during the COVID-19 outbreak in China, Science 17 Jun 2020: eabb7431, DOI: 10.1126/science.abb7431

Lelieveld, J., Evans, J. S., Fnais, M., Giannadaki, D., & Pozzer, A. (2015). The contribution of outdoor air pollution sources to premature mortality on a global scale. Nature, 525(7569), 367– 371. https://doi.org/10.1038/nature15371

Le Quéré, C., R. B. Jackson, M. W. Jones, A. J. P. Smith, S. Abernethy, R. M. Andrew, A. J. De-Gol, D. R. Willis, Y. Shan, J. G. Canadell, P. Friedlingstein, F. Creutzig and G. P. Peters: Temporary reduction in daily global CO_2 emisisons during the COVID-19 forced confinement. Nature Climate Change, https://doi.org/10.1038/s41558-020-0797-x, 2020.

Marécal, V., Peuch, V.-H., Andersson, C., Andersson, S., Arteta, J., Beekmann, M., Benedictow, A., Bergström, R., Bessagnet, B., Cansado, A., Chéroux, F., Colette, A., Coman, A., Curier, R. L., Denier van der Gon, H. A. C., Drouin, A., Elbern, H., Emili, E., Engelen, R. J., Eskes, H. J., Foret, G., Friese, E., Gauss, M., Giannaros, C., Guth, J., Joly, M., Jaumouillé, E., Josse,

Formatted: Font colour: Text 1

Formatted: Font: (Default) +Body (Times New Roman), 10 pt, Font colour: Text 1

Formatted: Left

Formatted

B., Kadygrov, N., Kaiser, J. W., Krajsek, K., Kuenen, J., Kumar, U., Liora, N., Lopez, E., Malherbe, L., Martinez, I., Melas, D., Meleux, F., Menut, L., Moinat, P., Morales, T., Parmentier, J., Piacentini, A., Plu, M., Poupkou, A., Queguiner, S., Robertson, L., Rouïl, L., Schaap, M., Segers, A., Sofiev, M., Tarasson, L., Thomas, M., Timmermans, R., Valdebenito, Á., van Velthoven, P., van Versendaal, R., Vira, J., and Ung, A.: A regional air quality forecasting system over Europe: the MACC-II daily ensemble production, Geosci. Model Dev., 8, 2777–2813, https://doi.org/10.5194/gmd-8-2777-2015, 2015.

Manuel A. Zambrano-Monserrate, María Alejandra Ruano, Luis Sanchez-Alcalde, Indirect effects of COVID-19 on the environment, Science of The Total Environment, Volume 728, 2020, 138813, ISSN 0048-9697, https://doi.org/10.1016/j.scitotenv.2020.138813.

~~Muhammad, S., X. Long, and M. Salman: COVID-19 pandemic and environmental pollution: A blessing in disguise? Science of the Total Environment, 728 (138820), https://doi.org/10.1016/j.scitotenv.2020.138820, 2020.~~

Myhre G. et al., "Anthropogenic and natural radiative forcing" in Climate Change 2013: The Physical Science Basis. Contribution of Working Group I to the Fifth Assessment Report of the Intergovernmental Panel on Climate Change, T. F. Stocker et al., Eds. (Cambridge University Press, Cambridge, United Kingdom, 2013), pp. 659–740.

Nakada, L. Y. K. and R. C. Urban: COVID-19 pandemic: Impacts on the air quality during the partial lockdown in Sao Paulo state, Brazil. Science of the Total Environment, 730 (139087), https://doi.org/10.1016/j.scitotenv.2020.139087, 2020.

Petetin, H., Bowdalo, D., Soret, A., Guevara, M., Jorba, O., Serradell, K., and Pérez García-Pando, C.: Meteorology-normalized impact of COVID-19 lockdown upon NO_2 pollution in Spain, Atmos. Chem. Phys. Discuss., https://doi.org/10.5194/acp-2020-446, in review, 2020.

Schiermeier. Q: Why pollution is falling in some cities but not others. Nature, 580 (7803), 313. https://doi.org/10.1038/d41586-020-01049-6, 2020.

Seinfeld, John H., and Spyros N. Pandis. 2006. *Atmospheric chemistry and physics: from air pollution to climate change*. Hoboken, N.J.: J. Wiley.

Veefkind, J. P., Aben, I., McMullan, K., Förster, H., de Vries, J., Otter, G., et al. (2012). TROPOMI on the ESA Sentinel-5 Precursor: A GMES mission for global observations of the atmospheric composition for climate, air quality and ozone layer applications. Remote Sensing of Environment, 120, 70–83. https://doi.org/10.1016/j.rse.2011.09.027

Wang, Y. Y. Yuan, Q. Wang, C. Liu, Q. Zhi, and J. Cao: Changes in air quality related to the control of coronavirus in China: Implications for traffic and industrial emissions. Science of the Total Environment, 731 (139133), https://doi.org/10.1016/j.scitotenv.2020.139133, 2020a.

Wang, Q. and M. Su: A preliminary assessment of the impact of COVID-19 on environment - A case study in China. Science of the Total Environment, 728 (138915), https://doi.org/10.1016/j.scitotenv.2020.138915, 2020b.

Worden, H. M., Edwards, D. P., Deeter, M. N., Fu, D., Kulawik, S. S., Worden, J. R., & Arellano, A. (2013). Averaging kernel prediction from atmospheric and surface state parameters based on multiple regression for nadir-viewing satellite measurements of carbon monoxide and ozone. Atmospheric Measurement Techniques, 6(7), 1633-1646. https://doi.org/10.5194/amt-6-1633-2013